

第1特集

3

# iPS細胞由来マスト細胞を用いた難治性疾患の新規治療薬開発へ向けて

独立行政法人医薬基盤研究所 山口 朋子、川端 健二

**Key words** マスト細胞 / iPS 細胞 / 創薬応用 / 炎症性腸疾患 / 多発性硬化症

## 幹細胞と iPS 細胞の違い

幹細胞は、様々な細胞へと分化する能力（多能性）を有しており、適切な条件下で培養することにより、血液細胞、神経細胞、心筋細胞など多種多様な細胞へと分化可能である。したがって、幹細胞は、薬効評価・安全性薬理試験などの創薬スクリーニングや再生医療への応用が期待されている（図1）。

幹細胞のなかでも、とくに人工多能性幹細胞すなわち iPS 細胞は、皮膚などの体細胞に数種の遺伝子を導入することにより樹立されることから、受精卵を用いる ES 細胞（胚性幹細胞）とは異なり、倫理的な問題を回避することができる。また、iPS 細胞は患者自身の細胞から樹立することができるため、移植細胞による拒絶反応の可能性が低いと考えられている。

iPS 細胞の応用においては、神経変性疾患であるパーキンソン病の患者から iPS 細胞を樹立し、目的の細胞に分化させることで、これまで技術的に不可能であっ



やまぐち ともこ  
**山口 朋子**

独立行政法人  
医薬基盤研究所

2010年、大阪  
大学大学院薬学

研究科博士後期課程修了。専門は免疫学。ES/iPS細胞から各種血液・免疫細胞への分化誘導法の確立、マスト細胞の分化・成熟化メカニズムの解明に向けて研究中。日本遺伝子治療学会H23年度アンジェスMG賞。[研究室リンク](#)



かわばた けんじ  
**川端 健二**

独立行政法人医薬基盤研究所  
大阪大学大学院薬学研究科

1997年、京都大学大学院薬学研究科博士後期課程薬学専攻修了（薬学博士）。大阪府立母子総合医療センター研究所免疫部門流動研究員、国立医薬品食品衛生研究所遺伝子細胞医薬部研究員などを経て、2005年、独立行政法人医薬基盤研究所 遺伝子導入制御プロジェクト主任研究員に。2010年より独立行政法人医薬基盤研究所幹細胞制御プロジェクトプロジェクトリーダー。専門は血液学。幹細胞の創薬応用を研究中。2012年 第10回産学官連携功労者表彰（厚生労働大臣賞）。[研究室リンク](#)

Author 著者

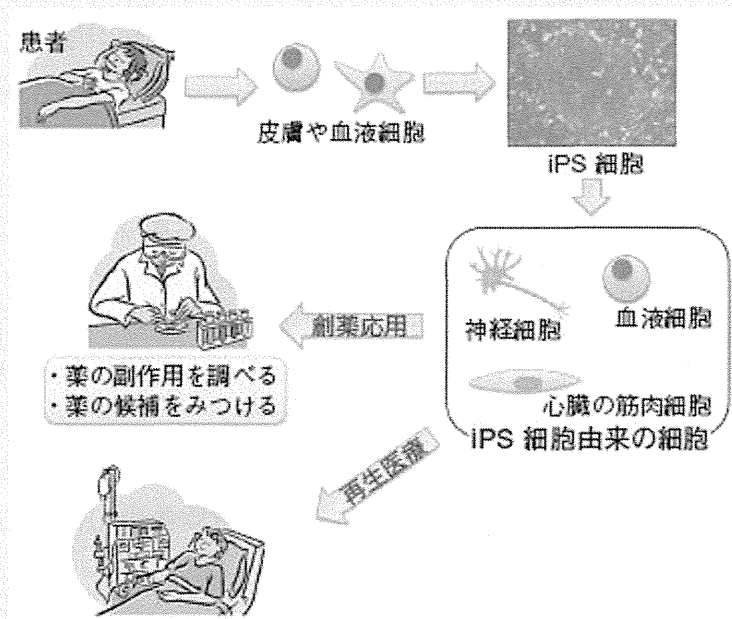


図1 iPS細胞を用いた臨床応用

た患者の体内組織（パーキンソン病であれば神経細胞）における病態を再現できることが報告されている<sup>1)</sup>。

また、アルツハイマー病の患者から樹立したiPS細胞を用いて、青魚に含まれる不飽和脂肪酸の一種がその発症を抑える可能性があることも報告されている<sup>2)</sup>。したがって、発症の原因が未だ不明な疾患のメカニズム解明や新規治療薬の開発に、患者由来iPS細胞が有用であることが示されている。他にも、進行性骨化性線維異形成症や原発性免疫不全症候群などの難治性疾患の患者からiPS細胞が樹立され、現在研究が進められている。

## 難治性疾患とマスト細胞

炎症性腸疾患は、長期にわたり消化管に原因不明の炎症を呈する難治性疾患であり、近年急速に罹患率が増加している。大腸の粘膜にびらんや潰瘍ができる潰瘍性大腸炎や大腸および小腸の粘膜の慢性の炎症、あるいは潰瘍ができるクローン病などは、炎症性腸疾患の代表的な疾患として知られている。

これらの疾患の病因は未だ明らかとなっておらず、現在では遺伝的因子と環境因子が複雑に絡み合っていると考えられている。



潰瘍性大腸炎やクローン病患者の腸管では、マスト細胞が増加していることから、マスト細胞がこれらの炎症性疾患の発症や増悪に関与していることが、かねてより示唆されていた。

マスト細胞は、蕁麻疹や花粉症といった即時型アレルギーにおいて刺激に応じてヒスタミンをはじめとする多様な炎症性メディエーター（起炎症性物質）を細胞外に放出することから、アレルギー応答における主要なエフェクター細胞<sup>\*1</sup>として機能することが知られている。しかし、即時型アレルギー以外におけるマスト細胞の生体内での役割については不明であり、現在少しずつ解明されている。近年、遺伝的にマスト細胞を欠損したマウス（C57BL/6<sup>W-sh/W-sh</sup> マウス）を用いて実験的に炎症性腸疾患を誘導したところ、野生型マウスと比較して炎症が軽減されることが報告されたことから、マスト細胞が炎症性腸疾患の病態の悪化に関与していることが示されている<sup>3)</sup>。

多発性硬化症は、脳や脊髄などの中枢神経系が炎症を起こすことにより、神経が障害される難治性疾患である。手足の麻痺や視力の低下などの重篤な症状が現れ、その症状は悪化と好転を繰り返すことを特徴とする。多発性硬化症の発症原因に関しては明らかになっていないが、近年の研究によりアレルギーや炎症性腸疾患だけでなく、多発性硬化症の発症や増悪にもマスト細胞が関与していることが示唆されている<sup>4)</sup>。実際、多発性硬化症の患者の脳に発現する遺伝子プロファイルを解析した研究では、ヒスタミン受容体、マスト細胞が有するプロテアーゼ、その他の炎症性メディエーターなど、マスト細胞由来の遺伝子やアレルギー炎症で発現が上昇する遺伝子の発現量が増加していることも報告されている。

## ES/iPS 細胞由来マスト細胞

前述したように、マスト細胞は種々の疾患の発症や増悪に関与していることが報告されていることから、これらの疾患においてマスト細胞を標的とした新規治療薬の開発が期待される。しかしながら、マスト細胞は、生体では皮膚等の組織に浸潤して存在しており、その数も少ないため生体から取り出して培養することは容易ではない。そこで我々は、iPS 細胞から効率良くマスト細胞を分化誘導可能な培養系の確立を試みた<sup>5)</sup>。iPS 細胞からマスト細胞を得るには、様々な血液細胞への分化能を有する血液前駆細胞、マスト細胞前駆細胞を分化誘導する必要がある。まず、マウス ES 細胞あるいは iPS 細胞から血液細胞を得る際に汎用され

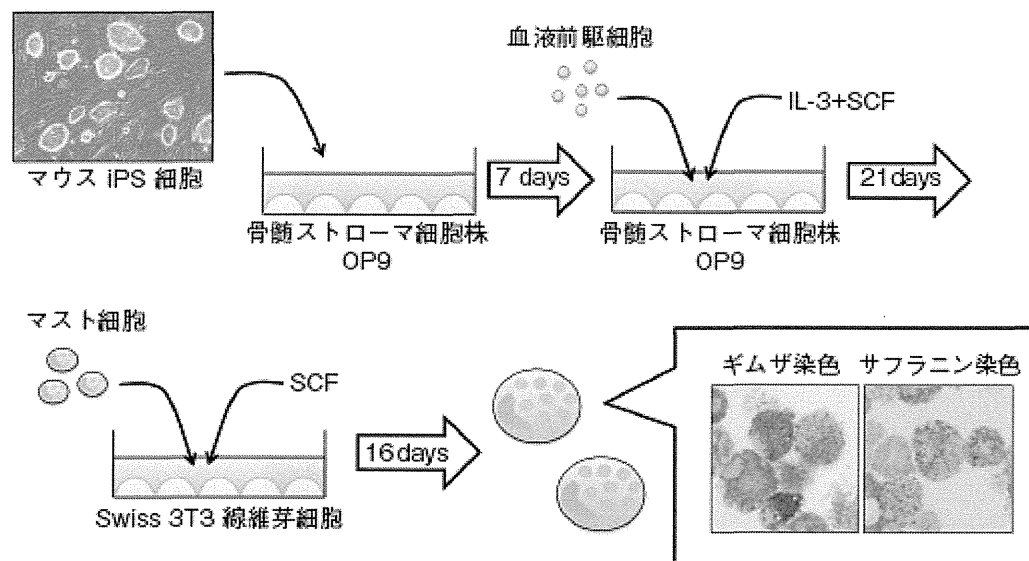


図2 iPS細胞からマスト細胞への分化誘導法

ている骨髓ストローマ細胞株である OP9 細胞と共培養することにより血液前駆細胞を誘導した。その後、マスト細胞への分化に有用とされているインターロイキン 3 (IL-3) や幹細胞増殖因子 (stem cell factor; SCF) 存在下で、血液前駆細胞を OP9 細胞と 21 日間共培養することでマスト細胞を得た (図 2)。得られた iPS 細胞由来マスト細胞は、マスト細胞研究で汎用されている IL-3 依存性骨髓由来マスト細胞と比較し、マスト細胞特異的酵素活性やマスト細胞の重要な機能である脱顆粒 (細胞内に蓄積している顆粒を刺激に応じて細胞外に放出する) 応答能の亢進が観察されたことから、より成熟度の高いマスト細胞であることが明らかとなった。さらに、得られた iPS 細胞由来マスト細胞を SCF 存在下で Swiss 3T3 線維芽細胞と共培養することで、生体に存在するマスト細胞と同様に、ヒスタミンなどの炎症性メディエーターを豊富に含む顆粒が多く存在するマスト細胞を分化誘導可能であることが示された (図 3)。

上述したように、炎症性腸疾患や多発性硬化症などの発症や悪化にマスト細胞が関与していることから、ヒト iPS 細胞由来マスト細胞を用いることで、これらの疾患に対してこれまでの治療薬とは作用点異なる新規治療薬の開発が可能となる。



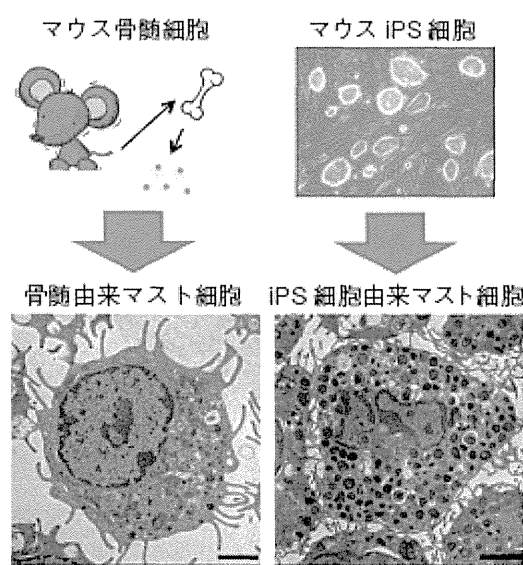


図3 iPS 細胞由来マスト細胞の表現型

マスト細胞のように、生体から取り出し培養することが困難な細胞は、iPS 細胞を用いた創薬応用に適した標的細胞であると考えられる。今後、ヒト iPS 細胞由来マスト細胞を効率良く分化誘導する方法が確立され、それを用いた難治性疾患の新しい治療薬が開発されることを期待している。

#### 【参考文献】

- 1) Imaizumi Y, et al: Mol Brain, 5, 35, 2012.
- 2) Kondo T, et al: Cell Stem Cell, 12, 487-496, 2013.
- 3) Kurashima Y, et al: Nat Commun, 3, 1034, 2012.
- 4) Steinman L, et al: Nat Immunol, 2, 762, 2001.
- 5) Yamaguchi T, et al: Stem Cells Dev, 22, 726-734, 2013.

#### 【用語解説】

- \*1 エフェクター細胞：T細胞のうち、細胞性抗体が反応に関係する遅延型アレルギー（Ⅳ型アレルギー）に関与するサイトカインを産生する細胞。

AU1►

# Two-Step Differentiation of Mast Cells from Induced Pluripotent Stem Cells

AU2► Tomoko Yamaguchi,<sup>1</sup> Katsuhisa Tashiro,<sup>1</sup> Satoshi Tanaka,<sup>2</sup> Sumie Katayama,<sup>3</sup> Waka Ishida,<sup>4</sup> Ken Fukuda,<sup>4</sup> Atsuki Fukushima,<sup>4</sup> Ryoko Araki,<sup>5</sup> Masumi Abe,<sup>5</sup> Hiroyuki Mizuguchi,<sup>1,6,7</sup> and Kenji Kawabata<sup>1,6</sup>

Mast cells play important roles in the pathogenesis of allergic diseases. They are generally classified into 2 phenotypically distinct populations: connective tissue-type mast cells (CTMCs) and mucosal-type mast cells (MMCs). The number of mast cells that can be obtained from tissues is limited, making it difficult to study the function of mast cells. Here, we report the generation and characterization of CTMC-like mast cells derived from mouse induced pluripotent stem (iPS) cells. iPS cell-derived mast cells (iPSMCs) were generated by the OP9 coculture method or embryoid body formation method. The number of Safranin O-positive cells, expression levels of CD81 protein and histidine decarboxylase mRNA, and protease activities were elevated in the iPSMCs differentiated by both methods as compared with those in bone marrow-derived mast cells (BMMCs). Electron microscopic analysis revealed that iPSMCs contained more granules than BMMCs. Degranulation was induced in iPSMCs after stimulation with cationic secretagogues or vancomycin. In addition, iPSMCs had the ability to respond to stimulation with the IgE/antigen complex *in vitro* and *in vivo*. Moreover, when iPSMCs generated on OP9 cells were cocultured with Swiss 3T3 fibroblasts, protease activities as maturation index were more elevated, demonstrating that mature mast cells were differentiated from iPS cells. iPSMCs can be used as an *in vitro* model of CTMCs to investigate their functions.

## Introduction

**M**AST CELLS HAVE recently gained attention, because they have been recognized as effector cells not only in allergic disorders, but also in other immune diseases, including autoimmune diseases and chronic inflammatory disorders [1]. Activation of mast cells triggers allergic and inflammatory responses through the release of a wide variety of mediators, such as histamine, arachidonic acid metabolites, and neutral proteases, and regulates immune responses through the production of cytokines and chemokines [2]. Mast cell precursors leave the bone marrow, migrate in the blood, invade tissues, and then proliferate and differentiate into mature cells [3]. Mature rodent mast cells are generally classified into 2 phenotypically distinct populations: connective tissue-type mast cells (CTMCs) and mucosal-type mast cells (MMCs) [3–4]. Each cell type differs with respect to location, staining characteristics, and histamine content. Mouse CTMCs, which are present in the peritoneal cavity and skin, contain heparin

and store large amounts of histamine. In contrast, mouse MMCs, which are prominent in the mucosal layer of the gastrointestinal tract, contain chondroitin sulfate E rather than heparin and have relatively low histamine content. Since recent studies have demonstrated that CTMCs are involved in a wide variety of immune responses [5–7], development of an *in vitro* culture system of CTMCs is needed. Although several mast cell lines and IL-3-dependent bone marrow-derived mast cells (BMMCs) have been used as models to investigate the process of mast cell activation and subsequent production of proinflammatory mediators, these models have limitations in analyzing the functions specific to mature mast cells. Previous studies showed that coculture of BMMCs with Swiss 3T3 fibroblasts in the presence of stem cell factor (SCF) facilitated morphological and functional maturation toward a CTMC-like phenotype [8].

Differentiation of both mouse and human embryonic stem (ES) cells into multiple hematopoietic lineages is now well established as a powerful tool for studying hematopoietic

<sup>1</sup>Laboratory of Stem Cell Regulation, National Institute of Biomedical Innovation, Osaka, Japan.

<sup>2</sup>Department of Immunobiology, Okayama University Graduate School of Medicine, Dentistry, and Pharmaceutical Sciences, Okayama, Japan.

<sup>3</sup>Bioresources Research, Laboratory of Common Apparatus, National Institute of Biomedical Innovation, Osaka, Japan.

<sup>4</sup>Department of Ophthalmology and Visual Science, Kochi Medical School, Kochi, Japan.

<sup>5</sup>Transcriptome Research Group, National Institute of Radiological Sciences, Chiba, Japan.

<sup>6</sup>Graduate School of Pharmaceutical Sciences, Osaka University, Osaka, Japan.

<sup>7</sup>The Center for Advanced Medical Engineering and Informatics, Osaka University, Osaka, Japan.

differentiation and lineage restriction, and for generating unlimited numbers of hematopoietic stem and progenitor cell populations for transplantation [9–12]. ES or induced pluripotent stem (iPS) cells into hematopoietic cells have been differentiated by embryoid body (EB) formation or coculture with stromal cells, such as OP9 cells [13–16]. By using these protocols, several groups have previously established methods to generate mast cells from mouse [17–19], cynomolgus monkey [20], and human [21] ES cells. ES cell-derived mast cells could respond to stimulation with antigen and substance P by releasing histamine. However, in most cases, these cells do not develop the large granules and high levels of proteolytic enzymes characteristic of tissue mast cells.

In this study, we generated mast cells from mouse iPS cells (iPSMCs), and characterized them from the point of view of morphology, function, and gene expression. Our results showed that the iPSMCs that were differentiated by coculture with OP9 stromal cells or the EB formation method had characteristics similar to CTMCs. When iPSMCs that were generated on OP9 cells were cocultured with Swiss 3T3 fibroblasts, the iPSMCs exhibited a more functional phenotype.

## Materials and Methods

### Cell cultures

Two mouse iPS cell clones, 38C2 (a kind gift from Dr. S. Yamanaka, Kyoto University, Kyoto, Japan) [22] and 2A-EGFPTg-4F-01 [23], were used in the present study. These mouse iPS cells were routinely cultured in a leukemia inhibitory factor-containing ES cell medium (Specialty Media) on mytomycin C-treated mouse embryonic fibroblasts (MEFs; Specialty Media), and they were passaged every 2 days using 0.25% trypsin-EDTA (Invitrogen). OP9 stromal cells were cultured in an  $\alpha$ -minimum essential medium ( $\alpha$ -MEM; Sigma) supplemented with 20% fetal bovine serum (FBS), 2 mM L-glutamine (Invitrogen), and 1  $\times$  nonessential amino acid (NEAA; Invitrogen).

### Generation of BMMCs

C57BL/6 mice were purchased from Nippon SLC. Bone marrow cells were prepared from the femurs and tibiae of mice. Cells were cultured in an RPMI 1640 medium containing 10% FBS, 1  $\times$  NEAA, and 10 ng/mL murine IL-3 (R&D Systems). The culture medium was replaced with a fresh medium every 5 days. After 4 weeks of culture, we confirmed the cellular surface expression of both Fc $\epsilon$ RI and c-kit (>95% positive).

### Differentiation of iPS cells to mast cells

Before coculturing with OP9 cells or EB formation, mouse iPS cells were suspended in an ES cell medium and cultured on a culture dish at 37°C for 30 min to remove MEF layers. In the OP9 cell-mediated differentiation method, iPS cells were transferred onto OP9 cells in 6-well plates at a density of  $1 \times 10^4$  cells per well. The induced cells were trypsinized on day 7, and  $1 \times 10^5$  cells were seeded onto fresh OP9 cells with  $\alpha$ -MEM supplemented with 20% FBS, 2 mM L-glutamine, 1  $\times$  NEAA, 30 ng/mL IL-3, and 100 ng/mL SCF (Peprotech).

After 7 days, nonadherent cells were reseeded onto fresh OP9 cells. The cells were subcultured every 7 days. We harvested the differentiated cells on day 28 and used them for further analysis.

In the EB-mediated differentiation method, iPS cell-derived EBs were generated by culturing iPS cells on a round-bottom low-cell-binding 96-well plate at  $1 \times 10^3$  cells per well. iPS cell-derived EBs were collected on day 7, and were transferred to a Petri dish with Differentiation Medium I [Dulbecco's modified Eagle's medium containing 15% FBS, 1  $\times$  NEAA, 2 mM L-glutamine, 1  $\times$  nucleosides, 0.1 mM 2-mercaptoethanol, penicillin/streptomycin, 30 ng/mL IL-3, 30 ng/mL IL-6 (Peprotech), and 100 ng/mL SCF]. After 7 days, nonadherent cells were transferred to a culture dish with Differentiation Medium II (Dulbecco's modified Eagle's medium containing 10% FBS, 1  $\times$  NEAA, 2 mM L-glutamine, penicillin/streptomycin, 30 ng/mL IL-3, and 100 ng/mL SCF). We harvested the nonadherent cells on day 28 and used them for further analysis.

### Transmission electron microscopy

BMMCs or iPSMCs were fixed with 2.5% glutaraldehyde in 0.1 M sodium phosphate buffer (pH 7.4), postfixed with 1% OsO<sub>4</sub>, dehydrated by a graded ethanol series, passed through QY-1 (Nisshin EM), and then embedded in Epon-812 (TAAB,). Ultrathin sections (0.06- $\mu$ m thick) were cut with an ultramicrotome (Leica Microsystems), stained with uranyl acetate-lead citrate, and observed using an electron microscope (H-7650, HITACHI) at 80 kV.

### Protease assay

BMMCs or iPSMCs were washed with phosphate-buffered saline (PBS), lysed in PBS containing 2 M NaCl/0.5% Triton X-100, and incubated for 30 min on ice. The lysate was centrifuged at 12,000 rpm for 30 min at 4°C. Activities of granule proteases in the resultant supernatants were measured using their specific chromogenic peptide substrates, such as S-2288 for tryptase (Sekisui medical) and M-2245 for carboxypeptidase A (CPA; Bachem) [24].

### $\beta$ -hexosaminidase release assay

$\beta$ -hexosaminidase activity was measured as a marker of the granular fraction for evaluation of degranulation. Cells were washed with an HEPES buffer (137 mM NaCl, 20 mM HEPES, 5 mM D-glucose, 2.7 mM KCl, 0.4 mM NaH<sub>2</sub>PO<sub>4</sub>, 0.5 mM MgCl<sub>2</sub>, 2.4 mM CaCl<sub>2</sub>, and 0.1% bovine serum albumin) and incubated with the buffer containing compound 48/80 (10  $\mu$ g/mL; Sigma) or substance P (100  $\mu$ M; Sigma) for 30 min. In the case of antigen stimulation, mast cells sensitized with 1  $\mu$ g/mL anti-dinitrophenyl (DNP) IgE (SPE7; Sigma-Aldrich) for 24 h were stimulated with 100 ng/mL DNP-human serum albumin (HSA; Biosearch Technologies) in the presence of lysophosphatidylserine (Lyso-PS; Avanti Polar Lipids).

### Coculture of mast cells with Swiss 3T3 fibroblasts

iPSMCs obtained after 28 days of culture with OP9 cells were cocultured with mitomycin C-treated Swiss 3T3 fibroblasts in the presence of 100 ng/mL SCF. BMMCs were

DIFFERENTIATION OF MAST CELLS FROM MOUSE IPS CELLS

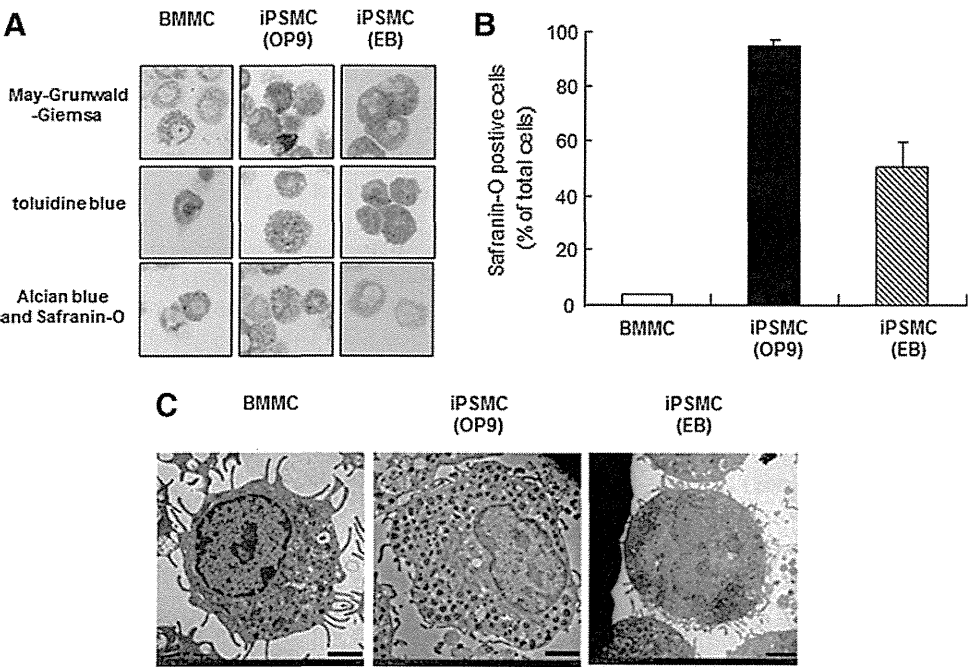


**FIG. 1.** Morphological characterization of induced pluripotent stem cell-derived mast cells (iPSMCs). **(A)** The iPSMCs, which were differentiated by coculture with OP9 cells or the embryoid body formation method, were harvested on day 28. Cyto-centrifuged preparations of bone marrow-derived mast cells (BMMCs) and the iPSMCs were stained with May-Grunwald-Giemsa, toluidine blue, or Alcian blue and Safranin O solutions. **(B)** The ratio of Safranin O-positive cells to total cells was calculated and shown as a percentage. The data represent the means  $\pm$  S.D. ( $n=4$ ). **(C)** BMMCs and iPSMCs were visualized by transmission electron microscopy. Scale bar = 2.0  $\mu$ m.

also cocultured with Swiss 3T3 fibroblasts under the same conditions. The subculture was performed every 4 days. The cells were trypsinized and replated, and nonadherent cells were collected as mast cells and used for further analysis.

*Mast cell reconstitution and induction of passive cutaneous anaphylaxis*

BMMCs or iPSMCs ( $5 \times 10^5$  cells) were injected subcutaneously into the conjunctivae of mast cell-deficient Kit<sup>W-sh/W-sh</sup>

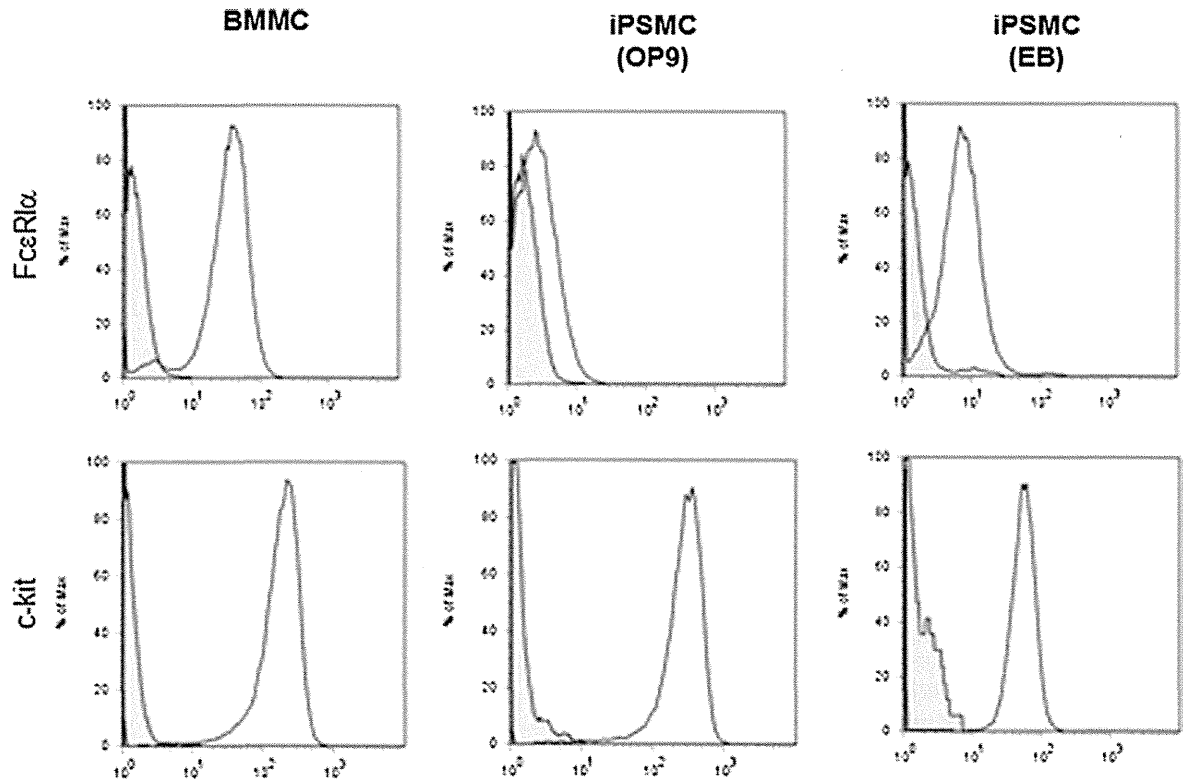


**FIG. 2.** Flow cytometric analysis of FcεRI and c-kit expression on iPSMCs. BMMCs and iPSMCs were stained with FITC-labeled anti-FcεRI and PE-labeled anti-c-kit antibodies for 30 min on ice. Stained cells were washed, resuspended in 1% fetal bovine serum-phosphate-buffered saline (FBS-PBS), and analyzed by flow cytometry.



mice. To elicit passive cutaneous anaphylaxis reactions, mice were injected subcutaneously into the conjunctiva with 75 ng anti-DNP IgE or saline. Then, 24 h after IgE injection, 100 µg DNP-HSA containing 2% Evan's blue dye was injected intravenously into mice. Thirty minutes later, the mice were killed, and their conjunctivae were excised. Evan's blue dye was extracted from conjunctivae with formamide, and the absorbance was measured at 610 nm.

Results

Generation of mast cells from mouse iPS cells

SF1 ► iPSMCs were generated by the OP9 coculture method or EB formation method as described in Supplementary Fig. S1 (Supplementary Data are available online at [www.liebertpub.com/scd](http://www.liebertpub.com/scd)). Approximately  $6.5 \times 10^6$  mast cells could be obtained from  $1 \times 10^5$  iPS cells by coculturing them with OP9 cells for 4 weeks. In addition, as in the case of BMMCs, iPSMCs can retain their proliferative potential (data not shown).

F1 ► Next, we performed the staining with May-Grunwald-Giemsa, toluidine blue, Alcian blue, and Safranin O solutions. May-Grunwald-Giemsa staining of the iPSMCs, which were differentiated by coculture with OP9 stromal cells or the EB formation method (Supplementary Fig. S1), revealed that induced mast cells gave rise to a uniform phenotype with rough basophilic granule-containing cells (Fig. 1A, upper). The granules in these cells showed a metachromatic staining pattern when stained with acid toluidine blue (Fig. 1A, middle). We then performed Alcian blue and Safranin O staining, by which mast cells are known to show a specific red color if they are CTMCs and a blue color if they are immature mast cells or MMCs [1]. While BMMCs were Alcian blue positive and Safranin O negative, iPSMCs were positive for both Alcian blue and Safranin O staining (Fig. 1A, [lower], B). Electron microscopic analysis revealed that the iPSMCs differentiated by either method contained more granules than BMMCs (Fig. 1C).

Expression of high-affinity IgE receptor on iPSMCs

F2 ► Mast cells are known to express c-kit and FcεRI (high-affinity IgE receptor) [1]. We next performed flow cytometric analysis to examine the surface expression of c-kit and FcεRI on iPSMCs. There was no significant difference in c-kit expression levels between iPSMCs and BMMCs (Fig. 2). In contrast, the FcεRIα expression level was significantly lower in the iPSMCs that were generated by coculture with OP9 cells, compared with that in BMMCs. Both c-kit<sup>+</sup>FcεRI<sup>+</sup> and c-kit<sup>+</sup>FcεRI<sup>-</sup> cells showed a granular phenotype by forward and side scatter (data not shown).

SF2 ► FcεRI is a heterotrimer composed of one α-chain and 2 γ-chains or a heterotetramer composed of one β-chain and 2 γ-chains. To evaluate the expression of each FcεRI subunit in iPSMCs, we analyzed mRNA expression levels by reverse transcription and quantitative polymerase chain reaction (RT-PCR). As shown in Supplementary Fig. S2, the expression levels of the mRNAs encoding the FcεRIα, FcεRIβ, and FcεRIγ chains were reduced in the iPSMCs differentiated by either method as compared with the levels in BMMCs.

Phenotypic differences between iPSMCs and BMMCs

To further compare the degree of mast cell differentiation, we measured the tryptase and CPA activities in iPSMCs. The tryptase and CPA activities were elevated in the iPSMCs derived from either method as compared with those in BMMCs (Fig. 3).

Histidine decarboxylase (HDC) is a critical enzyme that is involved in the synthesis of endogenous histamine in mammals [25–26], and is considered to be one of the indices of mast cell maturation [26]. Therefore, quantitative RT-PCR analysis was performed to compare the expression of HDC mRNA levels in iPSMCs and BMMCs (Supplementary Fig. S3). The expression level of HDC mRNA was elevated in the iPSMCs that were differentiated by either method as compared with that in BMMCs.

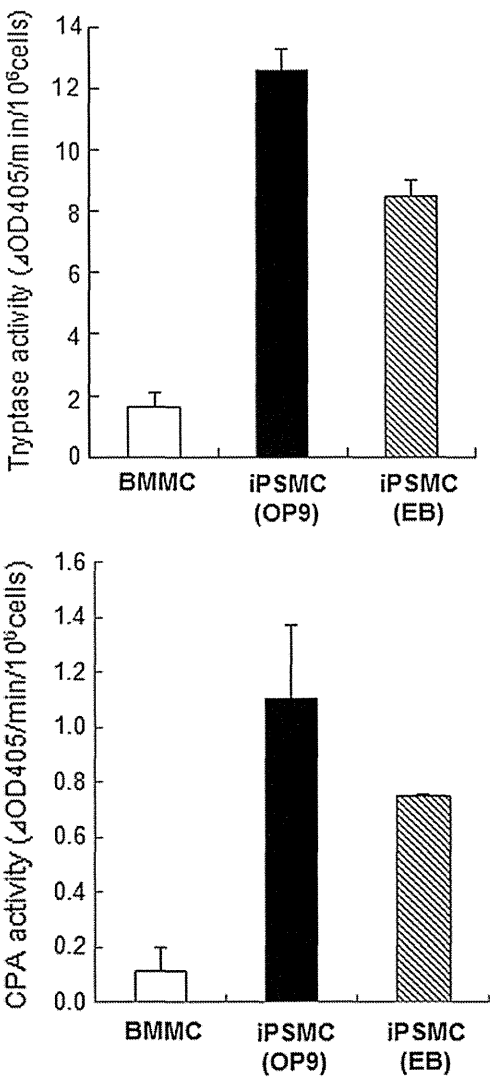
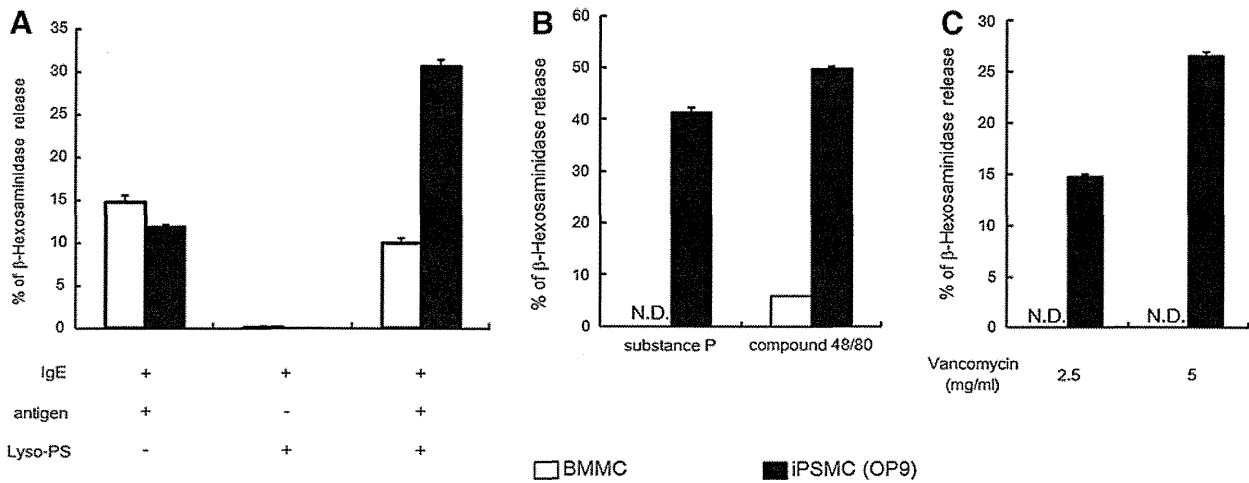


FIG. 3. Tryptase and carboxypeptidase A (CPA) activities in iPSMCs. Cell extracts prepared from BMMCs and iPSMCs were assayed for tryptase and CPA activities as described in the Materials and Methods section. All data represent the means ± S.D. (n = 4).

DIFFERENTIATION OF MAST CELLS FROM MOUSE IPS CELLS



**FIG. 4.**  $\beta$ -hexosaminidase release from iPSMCs after stimulation with IgE/antigen, compound 48/80, substance P, and vancomycin. **(A)** The exocytotic response was determined by measuring the release of  $\beta$ -hexosaminidase. BMMCs (open bar) and the iPSMCs that were cocultured with OP9 cells (closed bar) were sensitized with anti-dinitrophenyl (DNP) IgE and stimulated with DNP human serum albumin (HSA) in the presence or absence of Lyso-PS as described in the Materials and Methods section.  $\beta$ -hexosaminidase enzymatic activity was measured in supernatants and cell pellets solubilized with 0.5% Triton X-100 in HEPES buffer. **(B)** BMMCs (open bar) and the iPSMCs that were cocultured with OP9 cells (closed bar) were stimulated with compound 48/80 or substance P. **(C)** BMMCs (open bar) and the iPSMCs that were cocultured with OP9 cells (closed bar) were stimulated with vancomycin. All data represent the means  $\pm$  S.D. ( $n=3$ ).

Previously, Takano *et al.* demonstrated that *CD81*, a member of the tetraspanin superfamily, is one of the strikingly upregulated genes in BMMCs cocultured with Swiss 3T3 fibroblasts [8]. *CD81* is also considered to be a marker of CTMCs. FACS analysis showed that expression of *CD81* was elevated in the iPSMCs differentiated by either method as compared with that in BMMCs (Supplementary Fig. S4). In particular, our results revealed that the iPSMCs that were differentiated by coculture with OP9 cells were almost all *CD81* positive and showed a homogeneous population.

Degranulation of iPSMCs

We compared Fc $\epsilon$ RI-mediated degranulation of BMMCs and iPSMCs by measuring the extracellular activity of  $\beta$ -hexosaminidase, a marker enzyme for histamine-containing granules. As shown in Fig. 4A, the iPSMCs that were differentiated by coculture with OP9 cells displayed significantly less release of  $\beta$ -hexosaminidase than the BMMCs in response to IgE-mediated antigen stimulation. Similar results were obtained in iPSMCs that were derived from EB formation methods (Supplementary Fig. S5A). On the other hand, when the iPSMCs that were pretreated with anti-DNP monoclonal IgE were incubated with DNP-HSA in the presence of Lyso-PS, which is known to enhance IgE-mediated degranulation in rat peritoneal mast cells [27], the amount of  $\beta$ -hexosaminidase release was increased.

Responses to cationic secretagogues such as compound 48/80 and substance P are functional characteristics of CTMCs [4]. We next compared the IgE-independent responses between BMMCs and iPSMCs. Stimulation of iPSMCs with compound 48/80 resulted in marked exocytosis of  $\beta$ -hexosaminidase, whereas no or little release of this enzyme was detected from stimulated BMMCs (Fig. 4B and Supplementary Fig. S5B). Similarly,  $\beta$ -hexosaminidase release from

iPSMCs was much more markedly elevated by substance P treatment than  $\beta$ -hexosaminidase release from BMMCs (Fig. 4B and Supplementary Fig. S5B). In addition, stimulation of iPSMCs with vancomycin resulted in marked exocytosis of  $\beta$ -hexosaminidase, whereas no or little release of  $\beta$ -hexosaminidase was detected from vancomycin-stimulated BMMCs (Fig. 4C and Supplementary Fig. S5C). These results indicate that the iPSMCs display a CTMC-like phenotype.

Comparison between iPSMCs differentiated by the OP9 coculture and EB formation protocols

We next compared the degree of differentiation between the iPSMCs that were differentiated by the OP9 coculture method and those differentiated by the EB formation method. The expression level of Fc $\epsilon$ RI was significantly lower in the iPSMCs that were differentiated by coculture with OP9 cells as compared with the iPSMCs that were differentiated by EB formation (Fig. 2). However, the number of Safranin O-positive cells was significantly greater in the iPSMCs that were cocultured with OP9 cells than in the iPSMCs that were derived from the EB formation method (Fig. 1B). In addition, the expression levels of *HDC* mRNA and *CD81* protein were significantly higher in the iPSMCs that were cocultured with OP9 cells than in those that were derived from the EB formation method (Supplementary Figs. S3 and S4). These results showed that the iPSMCs that were cocultured with OP9 cells were more mature than the iPSMCs that were derived from the EB formation method. The iPSMCs that were derived from EB formation were more mature than BMMCs (Figs. 1–3). During the differentiation step, the iPSMCs that were derived from the EB formation method were designated as mast cells I (Fig. 5F). The iPSMCs that were differentiated by coculture with OP9 cells were also designated as mast cells II.

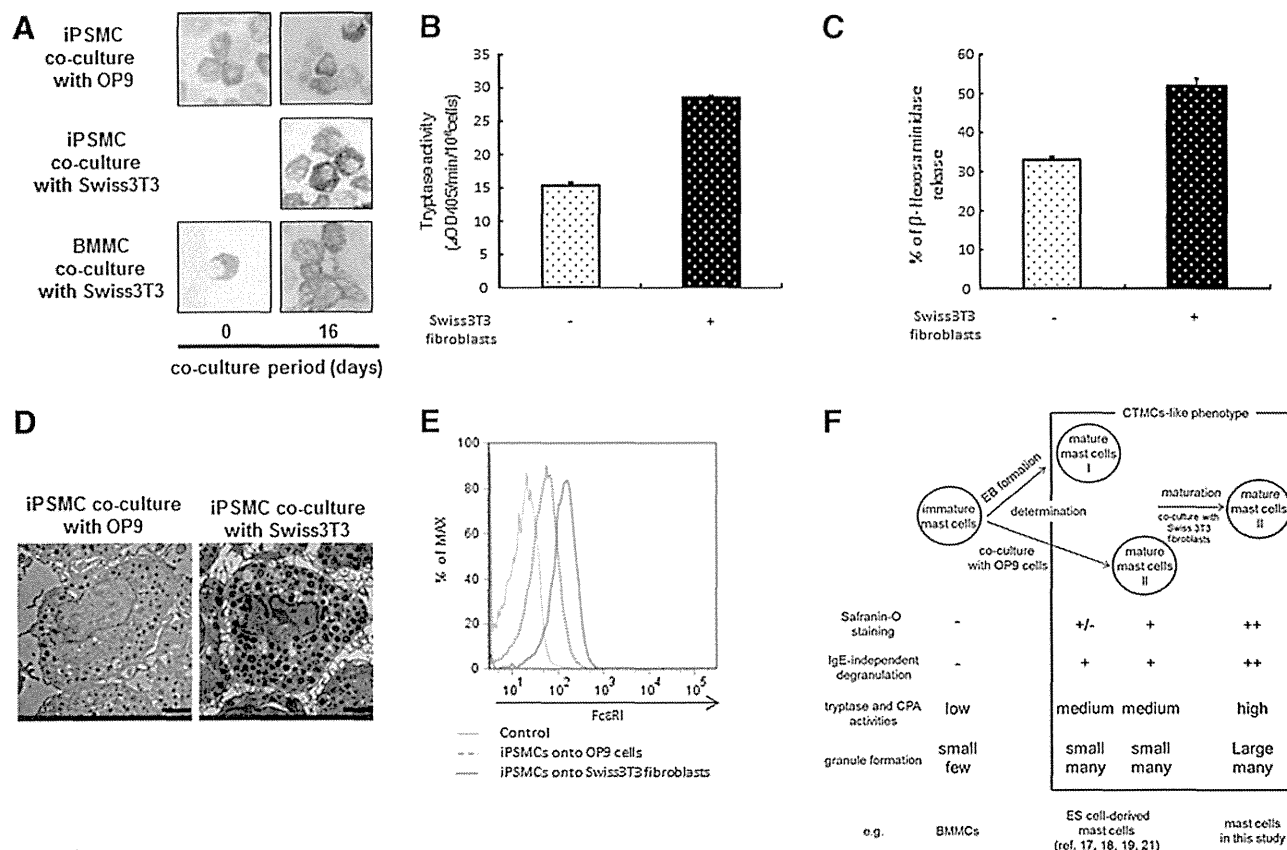


**FIG. 5.** Maturation of iPSMCs cocultured with Swiss 3T3 fibroblasts in the presence of stem cell factor. **(A)** Cyto-centrifuged preparations of the iPSMCs that were cocultured with OP9 cells or Swiss 3T3 fibroblasts, and the BMMCs that were cocultured with Swiss 3T3 fibroblasts were stained with Alcian blue and Safranin O. **(B)** Granule protease activities of the iPSMCs that were cocultured with OP9 cells or Swiss 3T3 fibroblasts were measured. **(C)** The exocytotic response was determined by measuring the release of  $\beta$ -hexosaminidase. The iPSMCs that were cocultured with OP9 cells (open bar) or Swiss 3T3 fibroblasts (closed bar) were stimulated with compound 48/80. **(D)** The iPSMCs that were cocultured with OP9 cells or Swiss 3T3 fibroblasts were analyzed by transmission electron microscopy. Scale bar = 2.0  $\mu$ m. **(E)** Suspensions of the iPSMCs that were cocultured with OP9 cells or Swiss 3T3 fibroblasts were stained with FITC-labeled anti-Fc $\epsilon$ RI antibody for 45 min on ice. The stained cells were washed, resuspended in 1% FBS-PBS, and analyzed by flow cytometry. **(F)** Scheme of 2-step differentiation of mast cells from iPS cells. All data represent the means  $\pm$  S.D. ( $n=3$ ).

### Enhancement of maturation in iPSMCs by Swiss 3T3 fibroblasts

A previous study reported that coculture of BMMCs with Swiss 3T3 fibroblasts in the presence of SCF facilitated morphological and functional maturation toward a CTMC-like phenotype [8]. It is possible that Swiss 3T3 fibroblasts promote the maturation of the iPSMCs (mast cells II) that are generated on OP9 cells. Therefore, we expected to generate more mature iPSMCs by coculturing with Swiss 3T3 fibroblasts. We compared the degree of mast cell maturation of the iPSMCs that were cocultured with OP9 cells or Swiss 3T3 fibroblasts. Although the majority of BMMCs were Alcian blue positive and Safranin O negative, the percentage of Safranin O-positive mast cells was gradually increased up to ~80% on day 16 after coculturing with Swiss 3T3 fibroblasts (Fig. 5A). The staining intensity for Safranin O on the iPSMCs that were cocultured with Swiss 3T3 fibroblasts was stronger than the iPSMCs (mast cells II) (Fig. 5A). Therefore,

the iPSMCs that were differentiated by coculture with Swiss 3T3 fibroblasts were found to be more mature than mast cells II and designated as mast cells III (Fig. 5F). We measured the tryptase activity in the iPSMCs (mast cells II) or iPSMCs (mast cells III), and found the elevated tryptase activity in the iPSMCs (mast cells III) relative to the iPSMCs (mast cells II) (Fig. 5B). Similarly,  $\beta$ -hexosaminidase release by compound 48/80 in the iPSMCs (mast cells III) was markedly elevated in comparison with that in the iPSMCs (mast cells II) (Fig. 5C). Electron microscopic analysis of mast cells revealed that the iPSMCs (mast cells III) contained more large granules (Fig. 5D). We performed flow cytometric analysis to examine the surface expression of c-kit and Fc $\epsilon$ RI on the iPSMCs (mast cells III). After coculturing, iPSMCs (mast cells III) and BMMCs still expressed similar levels of c-kit (data not shown). Remarkably, the expression level of Fc $\epsilon$ RI was elevated in the iPSMCs (mast cells III) (Fig. 5E). These results showed that there were 2 steps in iPSMC maturation process.

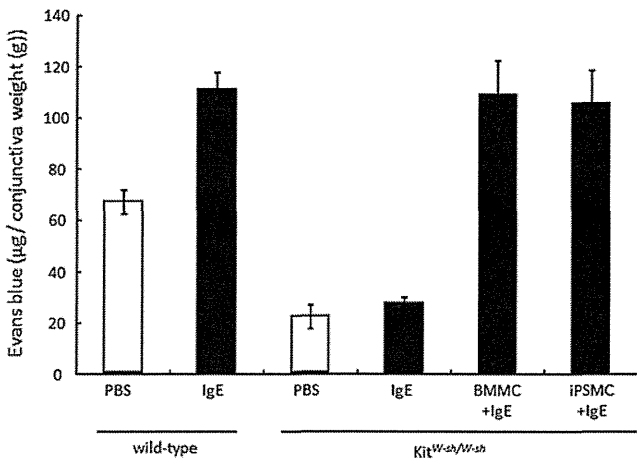


**FIG. 6.** IgE-dependent passive cutaneous anaphylaxis in mast cell-deficient Kit<sup>W-sh/W-sh</sup> mice reconstituted with iPSMCs. BMMCs or iPSMCs were injected subcutaneously into the conjunctivae of mast cell-deficient Kit<sup>W-sh/W-sh</sup> mice. After 6 weeks, mice were subcutaneously sensitized with anti-DNP IgE or saline, followed by induction of passive cutaneous anaphylaxis. After 24 h, mice were intravenously injected with DNP-HSA along with 2% Evan's blue dye. Thirty minutes later, conjunctivae were excised, and Evan's blue dye was extracted. Extravasation of Evan's blue dye was quantified as described in the Materials and Methods section. Results are normalized to average conjunctivae weight and are expressed as mean±S.D. (*n*=3 mice per group).

*Mast cell reconstitution and induction of passive cutaneous anaphylaxis*

We assessed whether the iPSMCs (mast cells I) with a C57BL/6 background could exhibit passive cutaneous anaphylaxis 6 weeks after injection of iPSMCs or BMMCs into the conjunctiva of mast-cell-deficient (Kit<sup>W-sh/W-sh</sup>) mice [28]. Kit<sup>W-sh/W-sh</sup> mice reconstituted with BMMCs or iPSMCs exhibited passive cutaneous anaphylaxis reactions in the conjunctivae as measured by extravasation of Evan's Blue dye (Fig. 6). On the other hand, no passive cutaneous anaphylaxis reactions in the conjunctivae were observed for Kit<sup>W-sh/W-sh</sup> mice that were not reconstituted with mast cells. These results indicate that iPSMCs had the ability to respond to stimulation with IgE/antigen *in vivo*.

**Discussion**

In this study, we developed a protocol consisting of mesoderm induction (stage 1), mast cell specification (stage 2), determination of mast cells (stage 3), and maturation of mast cells (stage 4) for mast cell differentiation from iPS cells

(Supplementary Figs. S1 and S6). BMMCs have been used extensively as a mast cell model. We compared the degree of maturation in BMMCs and iPSMCs. Expression level of CD81 was higher in the iPSMCs that were differentiated by both methods than in BMMCs (Supplementary Fig. S4). We also showed that IgE-mediated degranulation of iPSMCs was elevated in comparison with that in BMMCs in the presence of Lyso-PS (Fig. 4A and Supplementary Fig. S5A), demonstrating that iPSMCs were more mature than BMMCs. Therefore, both OP9 cells and EB-derived feeder cells might moderately promote the maturation of mast cells. The other possibility is that the maturation of iPSMCs might be accelerated by SCF. SCF is one of the most important cytokines for mast cell maturation [29]. BMMCs are in general generated without SCF. These are reasons why iPSMCs were more mature than BMMCs with respect to their phenotypes and functions.

Cytokines and feeder cells were required to induce the mast cell development from mouse iPS cells. As previously described, IL-3 is known to play an important role in mast cell specification. In contrast, BMMCs are generated without OP9 cells, suggesting that OP9 cells are not necessary for mast cell specification. OP9 cells might promote the maturation of mast cells, possibly by OP9 cell-derived factors, such as IL-4 [30–31], IL-6 [32–34], and nerve growth factor [34]. Therefore, cytokines and OP9 cells are all-essential and have distinct roles in the differentiation of mast cells from iPS cells.

We found a difference in FcεRI expression levels between iPSMCs (mast cell I) and iPSMCs (mast cell II) (Fig. 2). Surface expression level of FcεRI was lower in the iPSMCs (mast cells II), compared with that in the iPSMCs (mast cells I). More recently, Kovarova *et al.* reported that expression of FcεRIα mRNA was lower in human ES cell-derived mast cells that were cocultured with OP9 cells than in human ES cell-derived mast cells that were derived from the EB formation method [21]. These findings were fully consistent with our results. However, our results showed that iPSMCs (mast cells II) were more mature than iPSMCs (mast cells I). These results indicate that the expression levels of FcεRI are not completely correlated with the degree of mast cell differentiation, although the iPSMCs (mast cells III) showed a high level of FcεRI expression (Fig. 5E).

In the present study, we demonstrated that, as in the case of BMMCs, Swiss 3T3 fibroblasts could promote the maturation of iPSMCs (Fig. 5). A recent study has reported that cynomolgus monkey ES cells that are cocultured with the murine aorta-gonad-mesonephros-derived stromal cell line AGM-S1 cells are differentiated into CTMCs [20]. These results suggest that feeder cells, including AGM-S1 and Swiss3T3 fibroblasts, would promote mast cell maturation by similar mechanisms. These feeder cells might contribute

TABLE 1. PRIMER SEQUENCES (5'-3') FOR QUANTITATIVE REVERSE TRANSCRIPTION–POLYMERASE CHAIN REACTION

Genes	Sense primer	Antisense primer
HDC	CGCTCCATTAAGCTGTGGTTTGATTCGG	AGACTGGCTCCTGGCTGCTTGATGATCTTC
FcεRIα	GAGTGCCACCGTTCAAGACA	GTAGATCACCTTGCGGACATTG
FcεRIβ	TGGTTGGTTTGATATGCCTTTGT	CACTGCACCCAGAAATGGATA
FcεRIγ	ATCTCAGCCGTGATCTTGTCT	ACCATACAAAAACAGGACAGCAT

to the identification of factors that play a role in mast cell maturation.

While iPSMCs (mast cells II) were almost all Safranin O positive, iPSMCs (mast cells I) included both Safranin O-positive and negative populations, suggesting that immature cells were contained in iPSMCs (mast cells I). Expression levels of CD81 protein and HDC mRNA, and protease activities, were slightly elevated in the iPSMCs (mast cells II) as compared with the iPSMCs (mast cells I). Our results suggest that the iPSMCs (mast cells II) were more mature than iPSMCs (mast cell I). The iPSMCs (mast cells III) exhibited more mature phenotypes, such as large granules and high activity of protease. Taken together, the rank order of maturity in mast cells was the following: iPSMCs (mast cells III) > iPSMCs (mast cells II) > iPSMCs (mast cells I). The precise mechanisms of mast cell maturation process remain to be clarified. Classification of mast cells by using cell surface or internal marker can contribute to clarify the maturation mechanism of mast cells. Further studies are needed to find cell surface or internal marker that can clearly distinguish iPSMCs (mast cells I and II) and iPSMCs (mast cells III).

Our data demonstrate that iPSMCs could functionally respond to IgE stimulation *in vivo* (Fig. 6). There was no significant difference in Evan's blue extravasation in the Kit<sup>W-shi/W-shi</sup> mice reconstituted with iPSMCs or BMMCs. Previously, Fukuda *et al.* demonstrated that conjunctiva reconstituted with BMMCs display a CTMC-like phenotype [28]. Therefore, passive cutaneous anaphylaxis reactions were comparable in Kit<sup>W-shi/W-shi</sup> mice reconstituted with iPSMCs or BMMCs.

Galli's group first reported the identification of mast cell-committed progenitors (MCPs) in adult murine bone marrow [35]. They indicated that MCPs may be directly developed from multipotential progenitors independent of the myeloid pathway. In contrast, Arinobu *et al.* demonstrated that granulocyte/monocyte progenitors gave rise to MCPs [36]. The models of the developmental process in mast cells differed between these 2 reports. To analyze cells at each differentiation step, our differentiation protocol will be useful for clarifying the developmental process of mast cells.

Because of their pluripotency and self-renewal, ES cells and iPS cells are potential cell sources for regenerative medicine and other clinical applications, such as cell therapies, drug screening, toxicology, and investigation of disease mechanisms. Notably, iPS cell-based screening approaches might support the development of personalized medicine and tailor-made treatment plans. Vancomycin, an antibiotic to which methicillin-resistant *Staphylococcus aureus* (MRSA) is sensitive, frequently induces allergic reaction [37]. In this study, the stimulation of the iPSMCs with vancomycin resulted in marked exocytosis of  $\beta$ -hexosaminidase, whereas no or little release of this enzyme was detected from BMMCs (Fig. 4C and Supplementary Fig. S5C). Therefore, iPSMCs would be potential cell sources for drug-allergy-screening system.

We developed a 2-step differentiation protocol of mast cells from iPS cells. In the conventional method, CTMC-like mast cells are produced from bone marrow cells after 45 days of culture. In contrast, the iPSMCs generated on OP9 cells in the present study were produced after 28 days of culture. Thus, homogeneous CTMC-like mast cells can be easily generated from iPS cells by the OP9 coculture method. On the other hand, Swiss 3T3 coculture methods have different

advantage from OP9 coculture systems. The iPSMCs that were cocultured with Swiss 3T3 fibroblasts were more mature than the iPSMCs that were generated on OP9 cells. Because each of these methods has its advantages, the protocol should be chosen in accordance with the intended use.

We successfully developed a 2-step differentiation protocol for generating more mature mast cells from mouse iPS cells. The iPSMCs generated in this study exhibit many characteristics distinct from BMMCs. The iPSMCs possessed the characteristics of mature mast cells, including the heparin contents and degranulation, in response to cationic secretagogues and vancomycin. The iPSMCs serve as an excellent model for *in vitro* studies of CTMCs. Our results could facilitate clarification of the mechanisms that control the development of mast cells.

## Acknowledgments

We thank Dr. S. Yamanaka for kindly providing the mouse iPS cell lines 38C2. We would like to thank Misae Nishijima and Mary S. Saldon (National Institute of Biomedical Innovation) for technical assistance. We thank Dr. Keizo Nishikawa (National Institute of Biomedical Innovation) for helpful discussion.

## Author Disclosure Statement

The authors have no financial conflict of interest.

## References

1. Metcalfe DD, D Baram and YA Mekori. (1997). Mast cells. *Physiol Rev* 77:1033–1079.
2. Galli SJ, S Nakae and M Tsai. (2005). Mast cells in the development of adaptive immune responses. *Nat Immunol* 6:135–142.
3. Kitamura Y. (1989). Heterogeneity of mast cells and phenotypic change between subpopulations. *Annu Rev Immunol* 7:59–76.
4. Stevens RL and KF Austen. (1989). Recent advances in the cellular and molecular biology of mast cells. *Immunol Today* 10:381–386.
5. Benoist C and D Mathis. (2002). Mast cells in autoimmune disease. *Nature* 420:875–878.
6. Bryce PJ, ML Miller, I Miyajima, M Tsai, SJ Galli and HC Oettgen. (2004). Immune sensitization in the skin is enhanced by antigen-independent effects of IgE. *Immunity* 20:381–392.
7. Lu LF, EF Lind, DC Gondek, KA Bennett, MW Gleeson, K Pino-Lagos, ZA Scott, AJ Coyle, JL Reed, et al. (2006). Mast cells are essential intermediaries in regulatory T-cell tolerance. *Nature* 442:997–1002.
8. Takano H, S Nakazawa, Y Okuno, N Shirata, S Tsuchiya, T Kainoh, S Takamatsu, K Furuta, Y Taketomi, et al. (2008). Establishment of the culture model system that reflects the process of terminal differentiation of connective tissue-type mast cells. *FEBS Lett* 582:1444–1450.
9. Wang Y, F Yates, O Naveiras, P Ernst and GQ Daley. (2005). Embryonic stem cell-derived hematopoietic stem cells. *Proc Natl Acad Sci U S A* 102:19081–19086.
10. Karlsson KR, S Cowley, FO Martinez, M Shaw, SL Minger and W James. (2008). Homogeneous monocytes and macrophages from human embryonic stem cells following coculture-free differentiation in M-CSF and IL-3. *Exp Hematol* 36:1167–1175.



11. Ledran MH, A Krassowska, L Armstrong, I Dimmick, J Renstrom, R Lang, S Yung, M Santibanez-Coref, E Dzierzak, et al. (2008). Efficient hematopoietic differentiation of human embryonic stem cells on stromal cells derived from hematopoietic niches. *Cell Stem Cell* 3:85–98.
12. Murry CE and G Keller. (2008). Differentiation of embryonic stem cells to clinically relevant populations: lessons from embryonic development. *Cell* 132:661–680.
13. Nakano T, H Kodama and T Honjo. (1994). Generation of lymphohematopoietic cells from embryonic stem cells in culture. *Science* 265:1098–1101.
14. Chadwick K, L Wang, L Li, P Menendez, B Murdoch, A Rouleau and M Bhatia. (2003). Cytokines and BMP-4 promote hematopoietic differentiation of human embryonic stem cells. *Blood* 102:906–915.
15. Schmitt TM, RF de Pooter, MA Gronski, SK Cho, PS Ohashi and JC Zuniga-Pflucker. (2004). Induction of T cell development and establishment of T cell competence from embryonic stem cells differentiated in vitro. *Nat Immunol* 5:410–417.
16. Vodyanik MA, JA Bork, JA Thomson and II Slukvin. (2005). Human embryonic stem cell-derived CD34+ cells: efficient production in the coculture with OP9 stromal cells and analysis of lymphohematopoietic potential. *Blood* 105:617–626.
17. Tsai M, J Wedemeyer, S Ganiatsas, SY Tam, LI Zon and SJ Galli. (2000). In vivo immunological function of mast cells derived from embryonic stem cells: an approach for the rapid analysis of even embryonic lethal mutations in adult mice in vivo. *Proc Natl Acad Sci U S A* 97:9186–9190.
18. Sugiyama D, M Tanaka, K Kitajima, J Zheng, H Yen, T Murotani, A Yamatodani and T Nakano. (2008). Differential context-dependent effects of friend of GATA-1 (FOG-1) on mast-cell development and differentiation. *Blood* 111:1924–1932.
19. Wiles MV and G Keller. (1991). Multiple hematopoietic lineages develop from embryonic stem (ES) cells in culture. *Development* 111:259–267.
20. Ma F, N Kambe, D Wang, G Shinoda, H Fujino, K Umeda, A Fujisawa, L Ma, H Suemori, et al. (2008). Direct development of functionally mature tryptase/chymase double-positive connective tissue-type mast cells from primate embryonic stem cells. *Stem Cells* 26:706–714.
21. Kovarova M, AM Latour, KD Chason, SL Tilley and BH Koller. (2010). Human embryonic stem cells: a source of mast cells for the study of allergic and inflammatory diseases. *Blood* 115:3695–3703.
22. Okita K, T Ichisaka and S Yamanaka. (2007). Generation of germline-competent induced pluripotent stem cells. *Nature* 448:313–317.
23. Jincho Y, R Araki, Y Hoki, C Tamura, M Nakamura, S Ando, Y Kasama and M Abe. (2010). Generation of genome integration-free induced pluripotent stem cells from fibroblasts of C57BL/6 mice without c-Myc transduction. *J Biol Chem* 285:26384–26389.
24. Tchougounova E, G Pejler and M Abrink. (2003). The chymase, mouse mast cell protease 4, constitutes the major chymotrypsin-like activity in peritoneum and ear tissue. A role for mouse mast cell protease 4 in thrombin regulation and fibronectin turnover. *J Exp Med* 198:423–431.
25. Ohtsu H, A Kuramasu, S Tanaka, T Terui, N Hirasawa, M Hara, Y Makabe-Kobayashi, N Yamada, K Yanai, et al. (2002). Plasma extravasation induced by dietary supplemented histamine in histamine-free mice. *Eur J Immunol* 32:1698–1708.
26. Wiener Z, M Andrasfalvy, E Pallinger, P Kovacs, C Szalai, A Erdei, S Toth, A Nagy and A Falus. (2002). Bone marrow-derived mast cell differentiation is strongly reduced in histidine decarboxylase knockout, histamine-free mice. *Int Immunol* 14:381–387.
27. Hosono H, J Aoki, Y Nagai, K Bandoh, M Ishida, R Taguchi, H Arai and K Inoue. (2001). Phosphatidylserine-specific phospholipase A1 stimulates histamine release from rat peritoneal mast cells through production of 2-acyl-1-lysophosphatidylserine. *J Biol Chem* 276:29664–29670.
28. Fukuda K, M Ohbayashi, K Morohoshi, L Zhang, FT Liu and SJ Ono. (2009). Critical role of IgE-dependent mast cell activation in a murine model of allergic conjunctivitis. *J Allergy Clin Immunol* 124:827–833 e2.
29. Zsebo KM, J Wypych, IK McNiece, HS Lu, KA Smith, SB Karkare, RK Sachdev, VN Yuschenko, NC Birkett, et al. (1990). Identification, purification, and biological characterization of hematopoietic stem cell factor from buffalo rat liver—conditioned medium. *Cell* 63:195–201.
30. Yeatman CF, 2nd, SM Jacobs-Helber, P Mirmonsef, SR Gillespie, LA Bouton, HA Collins, ST Sawyer, CP Shelburne and JJ Ryan. (2000). Combined stimulation with the T helper cell type 2 cytokines interleukin (IL)-4 and IL-10 induces mouse mast cell apoptosis. *J Exp Med* 192:1093–1103.
31. Hamaguchi Y, Y Kanakura, J Fujita, S Takeda, T Nakano, S Tarui, T Honjo and Y Kitamura. (1987). Interleukin 4 as an essential factor for *in vitro* clonal growth of murine connective tissue-type mast cells. *J Exp Med* 165:268–273.
32. Hu ZQ, K Kobayashi, N Zenda and T Shimamura. (1997). Tumor necrosis factor- $\alpha$ - and interleukin-6-triggered mast cell development from mouse spleen cells. *Blood* 89:526–533.
33. Yuan Q, MF Gurish, DS Friend, KF Austen and JA Boyce. (1998). Generation of a novel stem cell factor-dependent mast cell progenitor. *J Immunol* 161:5143–5146.
34. Matsuda H, Y Kannan, H Ushio, Y Kiso, T Kanemoto, H Suzuki and Y Kitamura. (1991). Nerve growth factor induces development of connective tissue-type mast cells *in vitro* from murine bone marrow cells. *J Exp Med* 174:7–14.
35. Chen CC, MA Grimbaldston, M Tsai, IL Weissman and SJ Galli. (2005). Identification of mast cell progenitors in adult mice. *Proc Natl Acad Sci U S A* 102:11408–11413.
36. Arinobu Y, H Iwasaki, MF Gurish, S Mizuno, H Shigematsu, H Ozawa, DG Tenen, KF Austen and K Akashi. (2005). Developmental checkpoints of the basophil/mast cell lineages in adult murine hematopoiesis. *Proc Natl Acad Sci U S A* 102:18105–18110.
37. Horinouchi Y, K Abe, K Kubo and M Oka. (1993). Mechanisms of vancomycin-induced histamine release from rat peritoneal mast cells. *Agents Actions* 40:28–36.

Address correspondence to:

Dr. Kenji Kawabata

Laboratory of Stem Cell Regulation

National Institute of Biomedical Innovation

Saito-Asagi 7-6-8

Ibaraki, Osaka 567-0085

Japan

E-mail: kawabata@nibio.go.jp

Received for publication June 18, 2012

Accepted after revision October 8, 2012

Prepublished on Liebert Instant Online XXXX XX, XXXX

# Inhibition of Lnk in Mouse Induced Pluripotent Stem Cells Promotes Hematopoietic Cell Generation

Katsuhisa Tashiro,<sup>1,\*</sup> Miyuki Omori,<sup>1,2,\*</sup> Kenji Kawabata,<sup>1,3</sup> Nobue Hirata,<sup>1</sup> Tomoko Yamaguchi,<sup>1</sup> Fuminori Sakurai,<sup>2</sup> Satoshi Takaki,<sup>4</sup> and Hiroyuki Mizuguchi<sup>1,2,5</sup>

AU1►

AU2►

Embryonic stem (ES) cell- and induced pluripotent stem (iPS) cell-derived hematopoietic stem/progenitor cells (HSPCs) are considered as an unlimited source for HSPC transplantation. However, production of immature hematopoietic cells, especially HSPCs, from ES and iPS cells has been challenging. The adaptor protein Lnk has been shown to negatively regulate HSPC function via the inhibition of thrombopoietin (TPO) and stem cell factor signaling, and Lnk-deficient HSPCs show an enhanced self-renewal and repopulation capacity. In this study, we examined the role of Lnk on the hematopoietic differentiation from mouse ES and iPS cells by the inhibition of Lnk using a dominant-negative mutant of the Lnk (*DN-Lnk*) gene. We generated mouse ES and iPS cells stably expressing a DN-Lnk, and found that enforced expression of a DN-Lnk in ES and iPS cells led to an enhanced generation of Flk-1-positive mesodermal cells, thereby could increase in the expression of hematopoietic transcription factors, including *Scl* and *Runx1*. We also showed that the number of both total hematopoietic cells and immature hematopoietic cells with colony-forming potential in DN-Lnk-expressing cells was significantly increased in comparison with that in control cells. Furthermore, Lnk inhibition by the overexpression of the *DN-Lnk* gene augmented the TPO-induced phosphorylation of Erk1/2 and Akt, indicating the enhanced sensitivity to TPO. Adenovirus vector-mediated transient *DN-Lnk* gene expression in ES and iPS cells could also increase the hematopoietic cell production. Our data clearly showed that the inhibition of Lnk in ES and iPS cells could result in the efficient generation and expansion of hematopoietic cells.

## Introduction

SINCE EMBRYONIC STEM (ES) cells and induced pluripotent stem (iPS) cells can self-renew indefinitely and differentiate into all types of cells in the 3 germ layers, they are expected to have clinical applications in cell-based therapies [1–4]. For instance, ES cell- and iPS cell-derived hematopoietic cells are considered as an alternative source of adult hematopoietic cells for the treatment of hematological disorders and malignancies. Many groups have reported the differentiation of ES and iPS cells into mature hematopoietic cells, including erythrocytes, myeloid cells, and lymphoid cells [5–10]. However, previous reports have described the generation of only small numbers of mature hematopoietic cells, probably as a result of inefficient generation and expansion of immature hematopoietic cells derived from pluripotent stem cells. Therefore, the use of ES cell- and iPS cell-derived hematopoietic cells as a cell source for therapeutic applications de-

pends on the efficient production of hematopoietic cells, especially immature hematopoietic cells, from pluripotent stem cells.

Recently, inhibitors of differentiation (*ID*) genes, which are negative regulators of E proteins (E2A, HEB, and E2-2) [11], were shown to negatively regulate the hematopoietic differentiation in ES and iPS cells [12]. The same study also showed that the suppression of the ID genes, *ID1* and *ID3* increased the number of ES and iPS cell-derived hematopoietic progenitor cells [12]. These data indicate that negative regulators play an important role in the hematopoietic differentiation process in ES and iPS cells, and that manipulation of the expression of negative regulators would be an effective strategy for the efficient generation of hematopoietic cells from ES and iPS cells.

An adaptor protein Lnk/SH2B3 (hereafter referred to Lnk) is shown to negatively regulate the thrombopoietin (TPO) and stem cell factor (SCF) signaling, both of which are crucial

<sup>1</sup>Laboratory of Stem Cell Regulation, National Institute of Biomedical Innovation, Osaka, Japan.

<sup>2</sup>Laboratory of Biochemistry and Molecular Biology, Graduate School of Pharmaceutical Sciences, Osaka University, Osaka, Japan.

<sup>3</sup>Laboratory of Biomedical Innovation, Graduate School of Pharmaceutical Sciences, Osaka University, Osaka, Japan.

<sup>4</sup>Department of Immune Regulation, National Center for Global Health and Medicine, Research Institute, Tokyo, Japan.

<sup>5</sup>The Center for Advanced Medical Engineering and Informatics, Osaka University, Osaka, Japan.

\*These two authors contributed equally to this work.

cytokine-signaling pathways involved in hematopoietic stem cell (HSC) self-renewal, since Lnk-deficient HSCs exhibit an augmented response to TPO and SCF stimulation, and thereby Lnk-deficient mice show the marked HSC expansion in the bone marrow [13–16]. In addition, Lnk is highly expressed in immature hematopoietic cells, particularly in HSCs [17], in contrast to ID genes, which are ubiquitously expressed in many tissues [11,18]. Therefore, we speculated that an inhibition of Lnk function in ES and iPS cells would lead to the efficient generation and expansion of immature hematopoietic cells. In the present study, we investigated the effects of Lnk inhibition on the hematopoietic differentiation of mouse ES and iPS cells, and we found that a suppression of Lnk function by the enforced expression of a dominant-negative mutant of the Lnk (*DN-Lnk*) gene in ES and iPS cells resulted in an increase in the number of both mesodermal cells with hematopoietic differentiation potential and immature hematopoietic cells. These findings indicate that the suppression of the Lnk would be useful for the efficient generation and expansion of ES cell- and iPS cell-derived hematopoietic cells.

## Materials and Methods

### Plasmid construction and adenovirus vectors

pEF-IRESneo, which contains internal ribosome entry sites (IRES) and a neomycin-resistant gene (*Neo*) downstream of the human elongation factor (EF)-1 $\alpha$  promoter, was constructed by replacing the cytomegalovirus (CMV) promoter of pIRESneo (Clontech) with the EF-1 $\alpha$  promoter, which is derived from pEF/myc/nuc (Invitrogen). Mouse DN-Lnk cDNA, derived from pMY-DN-Lnk [19], was inserted into pEF-IRESneo, resulting in pEF-DN-Lnk-IRESneo. Adenovirus (Ad) vectors were constructed by an improved in vitro ligation method [20,21]. Mouse DN-Lnk cDNA was inserted into pHMCA5 [22], which contains the CMV enhancer/ $\beta$ -actin promoter with an  $\beta$ -actin intron (CA) promoter (a kind gift from Dr. J. Miyazaki, Osaka University) [23], resulting in pHMCA5-DN-Lnk. pHMCA5-DN-Lnk was digested with I-CeuI/PI-SceI and ligated into I-CeuI/PI-SceI-digested pAdHM4 [20], resulting in pAd-DN-Lnk. Ad-DN-Lnk and Ad-DsRed were generated and purified as described previously [24]. The CA promoter-driven  $\beta$ -galactosidase (LacZ)-expressing Ad vector, Ad-LacZ, and the CA promoter-driven DsRed-expressing Ad vector, Ad-DsRed, were generated previously [24,25]. The vector particle (VP) titer was determined using a spectrophotometric method [26].

### Cell culture

The mouse ES cell line, BRC6 (Riken Bioresource Center), and the mouse iPS cell line, 38C2 (a kind gift from Dr. S. Yamanaka, Kyoto University) [27], were used in this study. DN-Lnk- or *Neo*-expressing mouse ES and iPS cell lines were generated as follows. The pEF-IRESneo and pEF-DN-Lnk-IRESneo were linearized and were then electroporated into mouse ES cells and iPS cells by using Gene Pulser Xcell (250 V, 500  $\mu$ F; Bio-Rad Laboratory). pEF-IRESneo- or pEF-DN-Lnk-IRESneo-transfected ES cells and iPS cells were cultured in an ES cell medium containing 100  $\mu$ g/mL G418 (for ES cells) or 200  $\mu$ g/mL G418 (for iPS cells) for 10–14 days, and G418-resistant colonies were picked up and expanded.

The expression of DN-Lnk was confirmed by conventional reverse transcription-polymerase chain reaction (RT-PCR). Mouse ES cells, iPS cells, and *Neo*- or DN-Lnk-expressing mouse ES and iPS cells were cultured in a leukemia inhibitory factor-containing ES cell medium (Millipore) on mitomycin C-treated mouse embryonic fibroblasts (MEFs) [28]. OP9 stromal cells were cultured in an  $\alpha$ -minimum essential medium ( $\alpha$ -MEM; Sigma) supplemented with 20% fetal bovine serum (FBS), 2 mM L-glutamine (Invitrogen), and non-essential amino acid (Invitrogen).

### In vitro hematopoietic differentiation

For embryoid body (EB) differentiation, mouse ES and iPS cells were trypsinized and collected in an EB medium (EBM) containing the Dulbecco's modified Eagle's medium (Wako) supplemented with 15% FBS, non-essential amino acids (Millipore), penicillin/streptomycin (Invitrogen), 2 mM L-glutamine, and 100  $\mu$ M  $\beta$ -mercaptoethanol (Nacalai Tesque), and they were plated on a culture dish for 30 min to allow the MEFs to adhere. Nonadherent cells were collected and plated on a round-bottom Lipidure-coated 96-well plate (Nunc) at  $3 \times 10^3$  cells (ES cells) or  $1 \times 10^3$  (iPS cells) cells per well. On day 5, half of the medium was exchanged for fresh EBM. EBs were collected on day 7, and a single-cell suspension was prepared by the use of trypsin/ethylenediaminetetraacetic acid. The EB-derived cells ( $4 \times 10^5$  cells) were plated on OP9 stromal cells in the wells of a 6-well plate and were then cultured with an OP9 medium containing recombinant hematopoietic cytokines [100 ng/mL mouse SCF, 100 ng/mL human Flt3-ligand, 20 ng/mL mouse TPO, 5 ng/mL mouse interleukin (IL)-3, and 5 ng/mL human IL-6] to induce and expand the hematopoietic cells. In the case of DN-Lnk transduction using the Ad vector, EB-derived cells were transduced with Ad-LacZ or Ad-DN-Lnk at 3,000 VP/cell for 1.5 h in a 15-mL tube before the transduced EB-derived cells plating on OP9 cells. Hematopoietic cells were collected as described previously [25]. In brief, the floating and loosely attached cells were collected by pipetting and were transferred to 15-mL tubes. The adherent hematopoietic cells were harvested by trypsin treatment, and were then incubated in a tissue culture dish for 30–60 min to eliminate the OP9 stromal cells. Floating cells were collected as hematopoietic cells and transferred to the same 15-mL tubes. These hematopoietic cells were kept on ice for further analysis.

### Flow cytometry

The following primary monoclonal antibodies (Abs), conjugated with fluorescein isothiocyanate, phycoerythrin, or allophycocyanin, were used for flow cytometric analysis: anti-CD45 (30-F11; eBioscience), anti-CD11b (M1/70; eBioscience), anti-Sca-1 (D7; eBioscience), anti-Ter119 (Ter-119; eBioscience), anti-CD34 (RAM34; eBioscience), anti-CXCR4 (2B11; BD Bioscience), anti-Gr-1 (RB6-8C5; eBioscience), anti-c-Kit (ACK2 or 2B8; eBioscience), and anti-CD41 (MWR30; BD Bioscience). Purified rat anti-mouse c-Mpl/TPOR monoclonal Ab was obtained from IBL. Cells ( $1 \times 10^5$ – $5 \times 10^5$ ) were incubated with monoclonal Abs at 4°C for 30 min and washed twice with a staining buffer (phosphate-buffered saline/2% FBS). For detection of Mpl/TPOR, Dylight649-conjugated goat anti-rat IgG (BioLegend)

was used as a secondary Ab. After staining, the hematopoietic cells were analyzed and isolated by flow cytometry on an LSR II and FACSaria flow cytometer, respectively, using FACSDiva software (BD Bioscience).

Colony assay and May-Giemsa staining

The cells ( $5 \times 10^4$  cells) were cultured in a Methocult M3434 medium containing IL-3, IL-6, SCF, and erythropoietin (Stem-Cell Technologies, Inc.) for 10 days. The number of individual colonies was counted by microscopy. The colony number was normalized to the total number of hematopoietic cells. The multipotent hematopoietic progenitor cell-derived colonies (colony-forming unit-granulocyte, erythrocyte, monocyte, megakaryocyte (CFU-GEMM)/CFU-Mix) were picked up, fixed on glass slides using a cytospin centrifuge (Cytospin 4; Thermo Shandon), and stained with May-Grünwald Stain solution (Sigma) and Giemsa solution (Wako).

Western blotting

The adherent hematopoietic cells and OP9 stromal cells were collected, and were then incubated in a new tissue culture dish for 40 min to eliminate adherent OP9 cells. Floating cells were harvested and were subsequently starved in an RPMI1640 medium containing 0.1% FBS and penicillin/streptomycin for 4–6 h. Cells were stimulated with 20 ng/mL TPO for 10 min (for Jak2) or 30 min (for Erk and Akt) before being lysed in a lysis buffer [20 mM Tris-HCl (pH 8.0), 137 mM NaCl, 1% Triton X-100, 10% glycerol] containing a protease inhibitor cocktail (Sigma) and a phosphatase inhibitor cocktail (Nacalai Tesque). Cell lysates were loaded onto polyacrylamide gels and were transferred to a polyvinylidene fluoride membrane (Millipore). After blocking, the membrane was exposed to mouse anti-phospho-Erk1/2 (Cell Signaling), rabbit anti-Erk1/2 (Sigma), mouse anti-phospho-Akt (Cell Signaling), rabbit anti-total Akt (Cell Signaling), rabbit anti-phospho-Jak2 (Tyr1007/1008; Cell Signaling), or rabbit anti-Jak2 (Cell Signaling), followed by horseradish peroxidase-conjugated secondary antibody. The

band was visualized by ECL Plus Western blotting detection reagents (GE Healthcare) or Pierce Western Blotting Substrate Plus (Thermo Scientific), and the signals were read using an LAS-3000 imaging system (Fujifilm).

Reverse transcription–polymerase chain reaction

RT-PCR was carried out as described previously [25]. The sequences of the primers used in this study are listed in Table 1.

Results

Expression of Lnk in mouse ES and iPS cells

We initially investigated Lnk expression in mouse ES cells, iPS cells, ES cell-derived EBs (ES-EBs), and iPS-EBs. As shown in Fig. 1a, Lnk was expressed in undifferentiated ES and iPS cells, and the expression levels of Lnk were significantly increased after EB formation. We further examined whether Lnk was expressed in Flk-1-positive (+) cells, because hematopoietic cells were generated from Flk-1+ cells, a common hemoangiogenic progenitor during ES cell differentiation [29–31]. Quantitative RT-PCR analysis after the purification of Flk-1+ cells from ES-EBs and iPS-EBs revealed that Lnk was highly expressed in Flk-1+ cells (Fig. 1b). These data suggest that Lnk plays some role in the hematopoietic differentiation process in ES and iPS cells.

Enhanced mesodermal differentiation in EB by the inhibition of Lnk

The data described above led to the expectation that hematopoietic cells, including hematopoietic progenitor cells, could be efficiently generated from ES cells and iPS cells by the suppression of Lnk. To inhibit the function of Lnk, we utilized the DN-Lnk gene, which was developed by Takizawa et al. [19]. DN-Lnk binds to Lnk, and forms a multimer complex by a homophilic interaction with the N-terminal domain, thereby inhibiting Lnk function [19]. DN-Lnk-expressing ES and iPS cells were generated by introducing a

TABLE 1. LIST OF PRIMERS USED FOR REVERSE TRANSCRIPTION–POLYMERASE CHAIN REACTION

Gene name	(5') Sense primers (3')	(5') Antisense primers (3')
Gapdh	ACCACAGTCCATGCCATCAC	TCCACCACCCTGTTGCTGTA
Flk-1	TCTGTGGTTCTGCGTGGAGA	GTATCATTTCCAACCACCC
Lnk	GCCACTTTCTGCAGCTCTTC	GTCCAGGGAGTCAGTGCTTC
Lnk (for real-time)	AGCCACTTTCTGCAGCTCTTC	GTAGAGGTTGTCAGGCATCTCC
DN-Lnk	GGGCTACCAAGTGACACCAAT	CACTGTCCACGCTCTGTGAG
Oct-3/4	GTTTGCCAAGCTGCTGAAGC	TCTAGCCCAAGCTGATTGGC
Nanog	ATGGTCTGATTGAGAAGGGC	TTCACCTCCAAATCACTGGC
$\beta$ -H1	AGTCCCCATGGAGTCAAAGA	CTCAAGGAGACCTTTGCTCA
$\beta$ -major	CTGACAGATGCTCTCTTGGG	CACAACCCAGAAACAGACA
Scl/Tal-1	AACAACAACCGGGTGAAGAG	GGGAAAGCACGTCCTGTAGA
Runx1	CTTCCTCTGCTCCGTGCTAC	GACGGCAGAGTAGGGAAGTG
Gata1	TTGTGAGGCCAGAGAGTGTG	TTCTCTCGTGGATTCCATC
Gata2	TAAGCAGAGAAGCAAGGCTCGC	ACAGGCTTGCACAGGTAGTGG
Fli1	CCAACGAACGGAGAGTCATT	ATTTCCTTGCCATCCATGTTT
Erg	GGAGCTGTGCAAGATGACAA	GATTAGCAAGGCGGCTACTG
Erg (for real-time)	GGAGTGCAACCCTAGTCAGG	TAGCTGCCGTAGCTCATCC
Sfp11	CCATAGCGATCACTACTGGATT	TGTGAAGTGGTTCTCAGGGAAGT
E47	ATACAGCGAAGGTGCCCCACT	CTCAAGGTGCCAACACTGGT

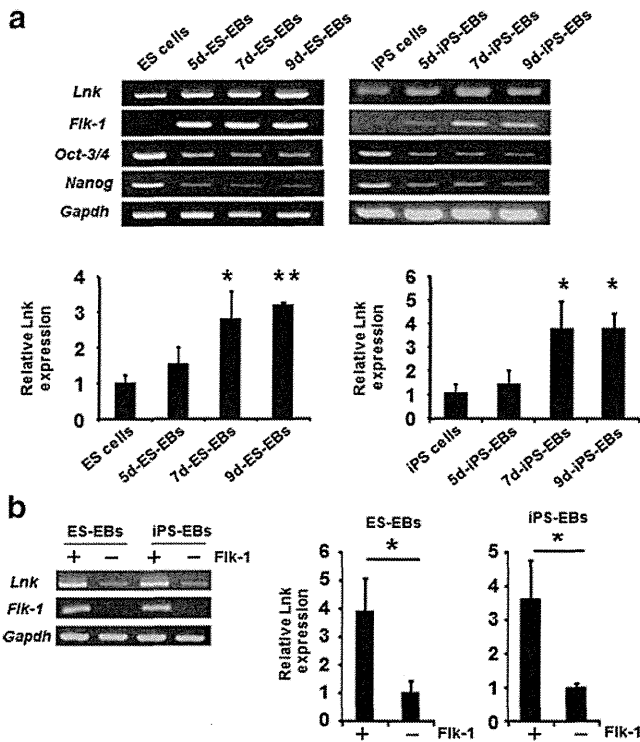


**FIG. 1.** Lnk is expressed in mouse ES cells, iPS cells, and Flk-1<sup>+</sup> hemoangiogenic progenitor cells. **(a)** Total RNA was extracted from undifferentiated ES cells, ES cell-derived EBs cultured for 5, 7, or 9 days (5-day ES-EBs, 7-day ES-EBs, 9-day ES-EBs, respectively), undifferentiated iPS cells, 5-day iPS-EBs, 7-day iPS-EBs, or 9-day iPS-EBs. Then, conventional (above) and quantitative (below) RT-PCR analysis was carried out. Results shown were the mean of 3 independent experiments with indicated SD. \**p* < 0.05, \*\**p* < 0.01 as compared with undifferentiated ES cells or iPS cells. **(b)** Flk-1<sup>+</sup> and Flk-1<sup>-</sup> cells were sorted from 7-day ES-EBs or 7-day iPS-EBs using FACS Aria. The purity of the Flk-1<sup>+</sup> and Flk-1<sup>-</sup> cells exceeded 90% and 95%, respectively (data not shown). Total RNA was extracted from both types of cell, and the expression of Lnk was examined by conventional (left) and quantitative (right) RT-PCR analysis. The data were expressed as mean ± SD (*n* = 3); \**p* < 0.05 as compared with Flk-1<sup>-</sup> cells. ES, embryonic stem; EBs, embryoid bodies; iPS, induced pluripotent stem; GAPDH, glyceraldehyde-3-phosphate dehydrogenase; RT-PCR, reverse transcription-polymerase chain reaction, SD, standard deviation.

Next, we generated EBs to induce mesodermal cells from DN-Lnk- or *Neo*-expressing ES and iPS cells. EBs were cultured for 7 days, because the proportion of Flk-1<sup>+</sup> cells in EBs increased to a peak on day 7, and decreased over the next 2 days in our culture conditions (Supplementary Fig. S2). We found that DN-Lnk-expressing cells on day 7 of the EB culture yielded a modest increase in the number of Flk-1<sup>+</sup> hemangiogenic progenitor cells relative to that of *Neo*-expressing cells (Fig. 2b). Interestingly, elevated expression of *Scl/Tal-1*, *Runx1*, and *Gata-1* was observed in DN-Lnk-expressing total EB cells (Fig. 2c). Besides the expression levels of these genes, those of other key transcription factors of blood stem/progenitor cells, including *Gata-2*, *Fli-1*, and *Erg* [32], in DN-Lnk-expressing cells were also upregulated in comparison with those in *Neo*-expressing cells (Fig. 2d). To examine whether increased expression of these transcription factors in DN-Lnk-expressing cells was due to the increased generation of Flk-1<sup>+</sup> cells, we performed the gene expression analysis after purification of Flk-1<sup>+</sup> cells from DN-Lnk- or *Neo*-expressing total EB cells (Fig. 2e). No difference in the expression of *Runx1*, *Gata-1*, *Gata-2*, *Fli-1*, or *Erg* was observed between DN-Lnk-expressing cells and *Neo*-expressing cells, indicating that elevated expression of these hematopoietic genes in DN-Lnk-expressing EB cells would be largely because of the increased population of Flk-1<sup>+</sup> cells. On the other hand, DN-Lnk-expressing Flk-1<sup>+</sup> cells showed a 2-fold increase in the expression of *Scl/Tal-1*, an essential transcription factor for the hematopoietic development [33,34], compared with *Neo*-expressing Flk-1<sup>+</sup> cells. The increased *Scl/Tal-1* expression thus suggests that an inhibition of Lnk in Flk-1<sup>+</sup> cells might contribute to enhance the production of hematopoietic progenitor cells. Taken together, these results raise the possibility that mesodermal cells with a hematopoietic differentiation potential would be efficiently generated in DN-Lnk-expressing cells during EB formation.

**Inhibition of Lnk function increases the production of hematopoietic cells**

To induce hematopoietic cells, EB-derived cells were cultured on OP9 stromal cells in the presence of hematopoietic cytokines. During culture, cobblestone-forming cells were more frequently observed in DN-Lnk-expressing cells than in *Neo*-expressing cells (Fig. 3a), indicating that DN-Lnk-expressing cells were immature hematopoietic cells with expansion potential. In support of this observation, DN-Lnk-expressing cells showed a significant increase in the number of hematopoietic cells compared to that of *Neo*-expressing cells (Fig. 3b). Importantly, compared to *Neo*-expressing cells, DN-Lnk-expressing cells could more efficiently proliferate on OP9 stromal cells for a period exceeding 14 days (Fig. 3b). Therefore, the proliferation of hematopoietic cells could be augmented by the inhibition of Lnk.

To investigate whether primitive and definitive hematopoiesis could occur in DN-Lnk- or *Neo*-expressing cells, we measured the expression levels of red cell globin by RT-PCR analysis. In both DN-Lnk- and *Neo*-expressing hematopoietic cells, the expression levels of the embryonic globin,  $\beta$ -H1, and the adult globin,  $\beta$ -major, were decreased and increased, respectively, after culturing on OP9 stromal cells in comparison with those in total EB cells (Fig. 3c). This indicates that DN-Lnk- or *Neo*-expressing cells can show the primitive

DN-Lnk-expressing plasmid, and DN-Lnk mRNA expression was confirmed by RT-PCR (Fig. 2a). In this report, we present data from one DN-Lnk-expressing ES and iPS cell clone, because the same results were obtained from other DN-Lnk-expressing clones. Notably, the expression levels of wild-type Lnk in DN-Lnk-expressing cells were similar to those in *Neo*-expressing cells and their parent cells (Fig. 2a). DN-Lnk-expressing iPS cells maintained the undifferentiated state in culture and possessed pluripotency, as demonstrated by alkaline phosphatase staining, immunostaining, and teratoma formation (Supplementary Fig. S1; Supplementary Data are available online at [www.liebertpub.com/scd](http://www.liebertpub.com/scd)). Hence, ectopic expression of the DN-Lnk gene in ES and iPS cells would not affect their function.



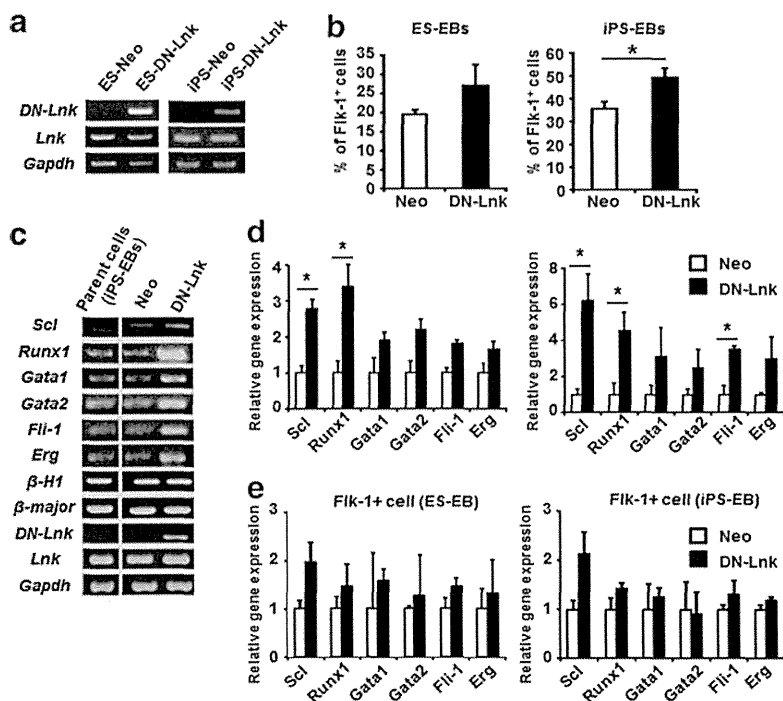


**FIG. 2.** Increased expression of hematopoietic transcription factors in DN-Lnk-expressing EB cells. **(a)** DN-Lnk-expressing ES cells and iPS cells were generated as described in the Materials and Methods section. DN-Lnk expression was confirmed by RT-PCR. **(b)** EB cells, which were cultured for 7 days, were stained with anti-mouse Flk-1 antibody, and were then subjected to flow cytometric analysis. The data were expressed as the mean  $\pm$  SD ( $n=3$ ). **(c)** The expression level of hematopoietic marker genes in 7-day iPS-EBs were investigated by semi-quantitative RT-PCR analysis. The *left panel* indicates the parent iPS cell (38C2)-derived 7-day EBs. **(d)** Gene expression analysis of the key transcription factors of hematopoietic stem/progenitor cells in total 7-day ES-EBs (*left*) and 7-day iPS-EBs (*right*). The data were expressed as mean  $\pm$  SD ( $n=3$ );  $*p < 0.05$  as compared with *Neo*. **(e)** After Flk-1<sup>+</sup> cells were sorted from *Neo*- or DN-Lnk-expressing 7-day EB cells, quantitative RT-PCR analysis was performed. *Left*, ES-EB-derived Flk-1<sup>+</sup> cells; *right*, iPS-EB-derived Flk-1<sup>+</sup> cells. DN-Lnk, dominant-negative mutant of the Lnk.

hematopoiesis followed by definitive hematopoiesis under our culture conditions.

We next examined the colony-forming potential of DN-Lnk-expressing cells. As shown in Fig. 3d, DN-Lnk-expressing cells showed a significant increase in the total colony-forming cell (CFC) number and CFU-granulocyte, macrophage number. Note that the number of CFU-GEMM/CFU-Mix, the most immature multipotent hematopoietic cells, in DN-Lnk-expressing cells was  $\sim 5$  times as much as that in *Neo*-expressing cells (Fig. 3d). May-Giemsa staining after picking up the colonies revealed that mixed colonies derived from DN-Lnk-expressing cells contained the erythroblasts, granulocytes, macrophages, and megakaryocytes (Fig. 3e), thus confirming the generation of multipotent hematopoietic cells. An elevated CFU-Mix number in DN-Lnk-expressing cells might have been due to the fact that Lnk is highly expressed in immature hematopoietic cells, especially in hematopoietic stem/progenitor cells [13,17]. We also analyzed surface antigen expression in DN-Lnk- or *Neo*-expressing cells by flow cytometry, and found that DN-Lnk-expressing cells showed a higher percentage of CD34<sup>+</sup> cells and CD41<sup>+</sup> cells (Fig. 3f), suggestive of an increased number of immature hematopoietic cells. In addition, the proportion of CD45<sup>+</sup> cells, CD11b<sup>+</sup> cells, Gr-1<sup>+</sup> cells, or CXCR4<sup>+</sup> cells was also increased in DN-Lnk-expressing cells (Fig. 3f). By contrast, a lower percentage of Ter119<sup>+</sup> cells were observed in DN-Lnk-expressing cells (Fig. 3f). Consistent with this flow cytometric analysis, we found an increased expression of *Sfp1* (encoding Pu.1) and *E47*, which are the key factors responsible for hematopoiesis, and a decreased expression of  $\beta$ -major globin in DN-Lnk-expressing cells after the cultivation on OP9 stromal cells (Fig. 3c and Supplementary Fig. S3). These results clearly showed that Lnk inhibition promoted the production of hematopoietic cells, including multipotent immature hematopoietic cells and myeloid cells, from mouse ES and iPS cells.

#### Inhibition of Lnk function in pluripotent stem cell-derived hematopoietic cells augments TPO-mediated signaling

It was previously shown that Lnk negatively regulates various types of hematopoietic cytokine signaling, such as TPO [16]. To investigate whether the increased production of hematopoietic cells from DN-Lnk-expressing cells, described above, is due to the enhanced TPO-mediated signaling, we analyzed protein phosphorylation after TPO stimulation using DN-Lnk-expressing cells. Hematopoietic cells were starved and subsequently stimulated with 20 ng/mL of TPO before the preparation of the cell lysates. The results showed the elevated phosphorylation of Jak2, Erk1/2, and Akt, all of which are downstream of TPO signaling, in DN-Lnk-expressing cells (Fig. 4a). We also found almost no difference in the percentage of Mpl/TPOR-positive cells between DN-Lnk-expressing cells and *Neo*-expressing cells (Fig. 4b), indicating that enhanced TPO signaling in DN-Lnk-expressing cells does not result from the increased percentage of Mpl/TPOR-expressing cells. Thus, our data suggest that Lnk inhibition by DN-Lnk gene transduction would augment the activation of signaling molecules upon stimulation with cytokines, and thus Lnk inhibition would promote the production of hematopoietic cells in DN-Lnk-expressing cells.

#### Increased generation of hematopoietic progenitor cells from mouse pluripotent stem cells by transient transduction of a DN-Lnk gene

Our groups have shown that Ad vector-mediated transient, but not constitutive, transduction of differentiation-related genes in pluripotent stem cells could result in the efficient generation of functional cells, such as adipocytes, osteoblasts, hepatocytes, and hematopoietic cells [25,28,35–37]. We expected that the transient inhibition of Lnk in iPS cells could also

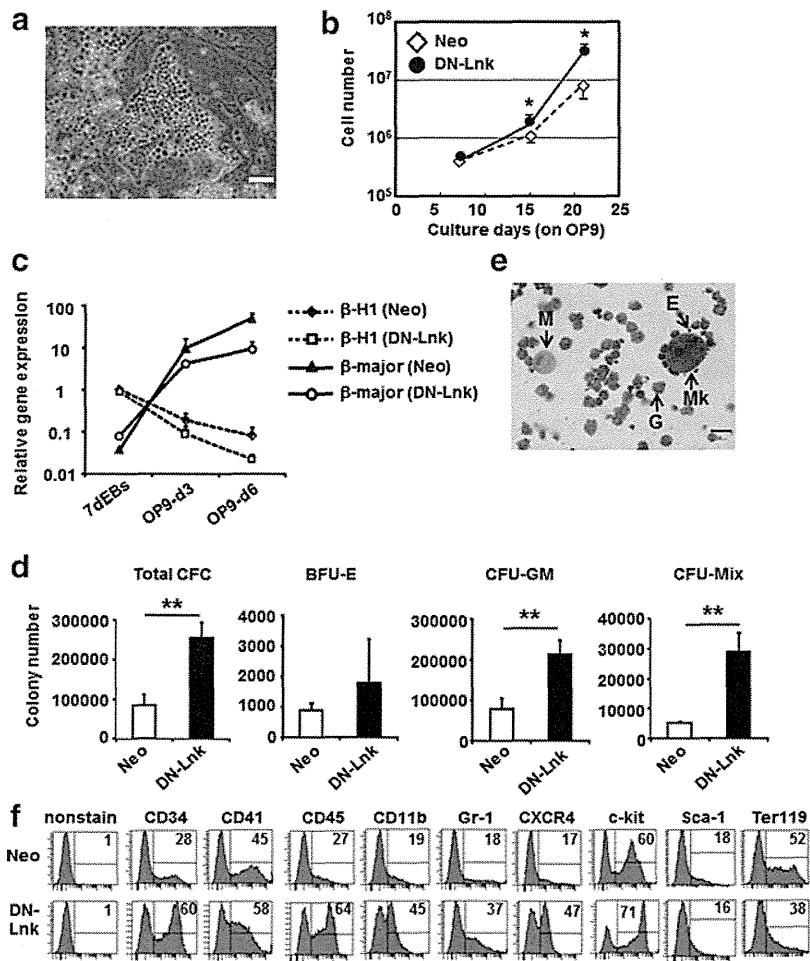


**FIG. 3.** Efficient generation of hematopoietic cells from iPS cells by overexpression of the *DN-Lnk* gene. EBs derived from *Neo*- or *DN-Lnk*-expressing iPS cells were cultured for 7 days, and were then plated and cultured on OP9 cells with hematopoietic cytokines to induce and expand the hematopoietic cells. **(a)** Morphology of cobblestone-forming cells derived from *DN-Lnk*-expressing cells on OP9 stromal cells. Scale bar indicates 100  $\mu$ m. **(b)** The number of hematopoietic cells was counted on days 7 and 14, after the EB cells were plated on OP9 cells. The data were expressed as mean  $\pm$  SD ( $n=3$ ); \* $p<0.05$  as compared with *Neo*. **(c)** Seven-day-cultured EB cells (7-day EBs) were cultured on OP9 cells for 3 or 6 days (OP9-d3 or OP9-d6, respectively). Total RNA was extracted from each cell, and the expression levels of the embryonic  $\beta$ -H1 globin and the adult  $\beta$ -major globin in the cells were measured by real-time PCR. **(d)** After the EB cells had been cultured on OP9 stromal cells for 7 days, the hematopoietic cells were cultured in a methylcellulose-containing medium with hematopoietic cytokines. Ten days later, the number of hematopoietic colonies was then determined using light microscopy. The number of total colonies or subdivided colonies (by morphological subtypes BFU-E, CFU-GM, and CFU-Mix) is shown. The colony number was normalized to the total number of cells. The data were expressed as mean  $\pm$  SD ( $n=3$ ); \* $p<0.05$  as compared with *Neo*. **(e)** Cytospin preparation from a *DN-Lnk*-expressing cell-derived CFU-Mix obtained from the cultures described in **(d)**. E, erythrocyte; G, granulocyte; M, macrophage; Mk, megakaryocyte. Scale bar indicates 30  $\mu$ m. **(f)** After the EB cells were cocultured with OP9 stromal cells for 14 days, the hematopoietic cells were collected as described in the Materials and Methods section. Hematopoietic cells derived from *Neo*- or *DN-Lnk*-expressing iPS cells were stained with each antibody, and were then subjected to flow cytometric analysis. The proportion of antigen-positive cells is indicated in the histograms. Representative results from 1 of 3 independent experiments performed are shown. CFC, colony-forming cell; BFU-E, burst-forming unit; CFU-GM, colony-forming unit-granulocyte and monocyte; CFU-Mix/CFU-GEMM, CFU-granulocyte, erythrocyte, monocyte, and megakaryocyte.\*\*

◀ AU4

accelerate the hematopoietic differentiation. To test this expectation, we generated a *DN-Lnk*-expressing Ad vector, Ad-*DN-Lnk*, and examined the effects of transient Lnk inhibition on hematopoietic cell differentiation. The transduction efficiency in EBs, which was transduced with a DsRed-expressing Ad vector, was approximately 40%, as determined by flow cytometry (data not shown). A colony assay after transduction with Ad vectors revealed that the number of total colonies and

mixed colonies in the cells transduced with Ad-*DN-Lnk* was slightly increased in comparison with that in the cells transduced with Ad-LacZ (control vector) (Fig. 5a, c). Moreover, the number of hematopoietic cells increased in Ad-*DN-Lnk*-transduced cells after 7-day cultivation on OP9 stromal cells (Fig. 5b, d). Thus, our data indicate that the transient inhibition of Lnk also enhances the differentiation and proliferation of hematopoietic cells derived from pluripotent stem cells.

◀ F5